



Cite this: *Nanoscale Adv.*, 2023, **5**, 596

Received 25th August 2022  
Accepted 15th December 2022

DOI: 10.1039/d2na00571a  
[rsc.li/nanoscale-advances](http://rsc.li/nanoscale-advances)

## 1 Introduction

Nature, through billions of years of evolution, has often provided unique but elegant designs and structures that have aided researchers and engineers to invent new technologies to enhance the capabilities of existing ones. The term 'biomimetics' or 'biomimicry', coined by American biophysicist O. H. Schmitt in the 1950s<sup>1,2</sup> is composed of two words that are derived from Greek words: 'bios' (meaning life) and 'mimesis' (meaning imitation). Biomimicry is the emulation of natural structures, designs, and elements with a view to develop novel devices with the desired functionalities.

<sup>a</sup>Department of Electrical and Electronic Engineering, Bangladesh University of Engineering and Technology, Dhaka 1205, Bangladesh. E-mail: [sajid@eee.buet.ac.bd](mailto:sajid@eee.buet.ac.bd)

<sup>b</sup>Department of Computer Science and Engineering, Brac University, 66 Mohakhali, Dhaka 1212, Bangladesh



*Mehedi Hasan Himel is a lecturer in the department of CSE, Brac University. He completed his BSc from the department of EEE, BUET, and is currently doing his MSc in the same department. His areas of research interest include 2D materials, molecular dynamics, and nanoelectronics.*



*Bejoy Sikder is a lecturer in the Department of EEE, BUET. He completed his BSc and is currently doing his MSc in the same department. His research interests include solid state electronics and optoelectronics.*



like a kingfisher's face to achieve better aerodynamics. We are now able to make wind turbines with improved energy efficiency and performance, thanks to the 'tubercles' (meaning large bumps) design found in humpback whales. Airplanes nowadays are designed like birds, and advanced robots are looking more and more like humans and animals. To push the limits of new innovations or to solve a complex engineering problem, humans have always looked at nature to seek answers.

Engineered biomimicry includes three methodologies: bio-inspiration, biomimetics, and bioreplication.<sup>3</sup> Bioinspiration is the implementation of an idea taken from nature without reproducing the actual structure or mechanism. For example, both helicopters and bumblebees hover, but the mechanisms are different. Biomimetics require the reproduction of the actual mechanism to obtain a certain functionality. Robots that walk on four or more legs are instances of biomimetics. However, the distinction between these two is very slight, and differentiating them is not always an easy task. The third approach, bioreplication is the direct replication of a biological structure to obtain a certain functionality. All these methodologies exploit natural instances to develop structures or devices with desirable functionalities.<sup>4</sup>

Biomimicry enables researchers to exploit natural solutions to solve a problem, and nanotechnology provides the methods for observing matters at a nanoscale level. Nanotechnology is the manipulation of matter at the nanometer ( $10^{-9}$  m) scale. It is one of the most promising technologies of this century, which has paved the way for many extraordinary innovations such as nano-sensors and nano-robots. There exists a close relationship between nanotechnology and biomimicry. All biological systems are comprised of units that are observed at the nanoscale, and biology inspires the creation of new devices and systems to enhance the capabilities of existing technology. Hence the integration of nanotechnology and biomimicry proves to be very essential in the amelioration of science and technology.

Although biomimicry in nanotechnology is a relatively new research direction, there are many excellent articles that go into

great depth to review the progress in the individual application domains of nanotechnology. Most recently, M. Simovic-Pavlovic *et al.* discussed the advancements of MEMS (micro-electromechanical systems) and NEMS (nanoelectromechanical systems), along with the trends in designing new nano-devices for advanced materials and sensing applications.<sup>5</sup> The clavate-hair-based sensory system of crickets has inspired a one-axis biomimetic MEMS accelerometer<sup>6</sup> and the lateral-line sensors of fish have inspired hydrodynamic flow sensor MEMS arrays, which are two of the most recent examples.<sup>7</sup> Biomimetic NEMS plays an important role in medicine. An inspiring advancement in this field was made in 2018 by Karthick *et al.*, who provided an improved insight into the blood plasma separation from whole blood within blood capillaries by using acoustophoresis, a natural phenomenon.<sup>8</sup> The lab-on-chip (LOC), an emerging technology with enormous potential in health and medicine, is also an instance of bioinspired nano-systems. As biomimetic MEMS do not fall into the scope of this paper, interested readers are encouraged to go through the excellent articles by F. Khoshnoud *et al.*,<sup>9</sup> M. Kruusmaa *et al.*,<sup>10</sup> J. Song *et al.*,<sup>11</sup> and A. Rahaman *et al.*<sup>12</sup> for applications in robotics, sensors, and audio technologies at the microscopic scale, respectively. P. P. Vijayan *et al.* discussed the scope of biomimetic functionalities such as self-healing, self-cleaning, *etc.*, for everyday materials.<sup>13</sup> L. Zhang *et al.* and E. S. Kim *et al.* discussed the advancements of biomimetic tissue engineering and regenerative nanomedicine in their review studies.<sup>14,15</sup> T. Li *et al.* and C. Guido *et al.* reviewed the recent progress of biomimetic cell membrane-coated nanoparticles and nanocarriers for cancer therapy.<sup>16,17</sup> Z. Jakšić *et al.* and A. Giwa *et al.* reviewed the development of biomimetic nano-membranes<sup>18,19</sup> while R. Bogue reviewed biomimetic nano-adhesives.<sup>20</sup> N. Soudi *et al.* reviewed biomimetic photovoltaic solar cells,<sup>21</sup> Y. Saylan *et al.* reviewed biomimetic molecular recognition and biosensing,<sup>22</sup> and S. Rauf *et al.* reviewed biomimetic optical nanosensors.<sup>23</sup> While many accomplished researchers and scientists of different fields have reviewed biomimicry in nanotechnology in specific application areas, to our knowledge, there exists no comprehensive review of biomimicry in the general field



*Tanvir Ahmed is a lecturer in the department of CSE, Brac University. He completed his BSc and is currently doing his MSc in the department of EEE, BUET. His research interests include signal processing, computer vision, and deep learning.*



*Sajid Muhammin Choudhury is working as an assistant professor in the Department of EEE, BUET. He completed his PhD from the School of Electrical and Computer Engineering in Purdue University. He is currently working on plasmonic biosensors, photonic communication tools, and quantum computing. He is the secretary of the IEEE Bangladesh Section, founding chair, IEEE Photonics Society Bangladesh Chapter and founding chair, The Optica (formerly OSA) Bangladesh Section. He is a senior member of the IEEE and member of Optica.*



Table 1 Overview

Fields	Applications	Biological inspiration	Significant instances	Features
Nano-sensor	Optical nanosensor	<ul style="list-style-type: none"> <li>• Built-in IR sensing capabilities of snakes and vampire bats<sup>24</sup></li> <li>• Wide field-of-view of the common housefly<sup>25</sup></li> <li>• Camouflage capabilities of cephalopods<sup>26</sup></li> <li>• Peptide bonds</li> </ul>	<ul style="list-style-type: none"> <li>• Heat sensors<sup>27</sup></li> <li>• Aircraft wing deflection measurement sensor<sup>25</sup></li> <li>• Vapor sensors<sup>28</sup></li> </ul>	<ul style="list-style-type: none"> <li>• Temperature sensing</li> <li>• Chemical sensing</li> <li>• Light weight</li> <li>• Low cost</li> <li>• Better form factor</li> </ul>
	Peptide nanosensor			<ul style="list-style-type: none"> <li>• Linking peptides to nanosensors</li> </ul>
	Tactile nanosensor	<ul style="list-style-type: none"> <li>• Human skin neuroreceptors</li> <li>• Venus flytrap</li> </ul>	<ul style="list-style-type: none"> <li>• Skin attachable adhesives or E-skins<sup>30</sup></li> <li>• Thermo-responsive self-folding microgrippers<sup>31</sup></li> </ul>	<ul style="list-style-type: none"> <li>• Reversible adhesion<sup>30</sup></li> <li>• Ease of deformability<sup>30</sup></li> <li>• Self-actuating action without any external power sources<sup>31</sup></li> <li>• Contains stimuli responsive hydrogel/polymers<sup>32</sup></li> <li>• Self-assembling nanostructured gel<sup>33</sup></li> <li>• Creates scaffolds that replicate natural tissues<sup>33-37</sup></li> </ul>
	Stimuli responsive nanosensor			
Nano-medicine	Tissue engineering	<ul style="list-style-type: none"> <li>• Human bone extracellular matrix (ECM)</li> <li>• Extracellular matrix proteins<sup>33-37</sup></li> <li>• Native tissue ECM<sup>38</sup></li> </ul>	<ul style="list-style-type: none"> <li>• Generation of bony tissues<sup>33</sup></li> <li>• Cell attachment, proliferation, differentiation and ultimately tissue generation</li> <li>• Hydrogels maintain the cell structure, repair bonds<sup>38,39</sup></li> </ul>	<ul style="list-style-type: none"> <li>• Hydrogels provide strong mechanical support<sup>40</sup> and adjust themselves to match the shape of the injury<sup>38</sup></li> <li>• Recovering tissues lost due to injury<sup>41</sup></li> </ul>
	Surgery	<ul style="list-style-type: none"> <li>• Reconstruction of tissues</li> </ul>	<ul style="list-style-type: none"> <li>• Vascularized composite tissue allotransplantation (VCA)<sup>41</sup></li> <li>• Tissue engineering</li> </ul>	
	Nanoparticles	<ul style="list-style-type: none"> <li>• Encapsulation of dendritic cells<sup>42</sup></li> <li>• Nanocage</li> </ul>	<ul style="list-style-type: none"> <li>• Encapsulation of internal influenza proteins on the VLPs<sup>42</sup></li> <li>• Protein cage nanoparticle, encapsulin<sup>44</sup></li> </ul>	<ul style="list-style-type: none"> <li>• Mimicking virus properties increased vaccine effectiveness<sup>43</sup></li> <li>• Protein based nanocages to deliver drugs to specific sites of the human body<sup>44</sup></li> </ul>
Nano-robots	Bacteria inspired nanorobots	<ul style="list-style-type: none"> <li>• Bacteria<sup>45</sup></li> </ul>	<ul style="list-style-type: none"> <li>• Self-assembled flagellar nanorobotic swimmers<sup>45</sup></li> </ul>	<ul style="list-style-type: none"> <li>• Imitates the rotary motion of helical bacteria flagella for propulsion<sup>45</sup></li> </ul>
	Platelet-camouflaged nanorobots	<ul style="list-style-type: none"> <li>• Hybrid red blood cells<sup>46</sup> and platelets<sup>45</sup></li> </ul>	<ul style="list-style-type: none"> <li>• Flagellar nano-swimmers<sup>47</sup></li> </ul>	<ul style="list-style-type: none"> <li>• Platelet imitating properties like binding to toxins or special kinds of pathogens<sup>46</sup></li> <li>• Anthocyanin to recreate photosynthesis<sup>48,49</sup></li> <li>• Thin photovoltaic film converts light into energy<sup>50</sup></li> <li>• Increase in the optical path length <i>via</i> light trapping<sup>52</sup></li> <li>• Wide angular field and decreases the reflectance<sup>53,54</sup></li> <li>• Replicates the gentle sway of kelps<sup>60</sup></li> </ul>
Nano energy harvest	Solar energy	<ul style="list-style-type: none"> <li>• Photosynthesis</li> <li>• Plant leaves<sup>48</sup></li> <li>• Butterfly wings<sup>52</sup></li> <li>• Compound eye of insects<sup>53,54</sup></li> </ul>	<ul style="list-style-type: none"> <li>• Gratzel cell<sup>49,50</sup></li> <li>• Nanoleaves and nano trees<sup>51</sup></li> <li>• Solar energy harvesting<sup>52,53</sup></li> </ul>	<ul style="list-style-type: none"> <li>• Increase of external quantum and power conversion efficiencies of solar cells</li> <li>• Incident angle and polarization independent reflectance</li> </ul>
	Ocean energy	<ul style="list-style-type: none"> <li>• Kelp</li> </ul>	<ul style="list-style-type: none"> <li>• Bio-inspired triboelectric nanogenerator (BITENG)<sup>55-59</sup></li> <li>• Integration of moth-eye nanostructures into solar cells<sup>61-74</sup></li> </ul>	
Nano-photonics	Anti-reflecting coating	<ul style="list-style-type: none"> <li>• Moth-eye</li> </ul>	<ul style="list-style-type: none"> <li>• Superhydrophobic surface in foldable displays<sup>74</sup></li> </ul>	



Table 1 (Contd.)

Fields	Applications	Biological inspiration	Significant instances	Features
Textile engineering	Anti-reflective transparent nanostrcutures	<ul style="list-style-type: none"> <li>Transparent wings of <i>Greta Oto</i></li> <li>Cicada <i>Cretensis</i><sup>75-77</sup></li> </ul>	<ul style="list-style-type: none"> <li>Omnidirectional anti-reflective glass<sup>78</sup></li> </ul>	<ul style="list-style-type: none"> <li>Foldable displays exhibit excellent mechanical resilience with good thermal and chemical resistance</li> <li>Less than 1% reflectivity irrespective of the angle of incidence for S-P linearly polarized light</li> </ul>
	Water repellent textiles	<ul style="list-style-type: none"> <li>Lotus leaf<sup>79-83</sup></li> </ul>	<ul style="list-style-type: none"> <li>Superhydrophobic surfaces on cotton textiles<sup>84</sup></li> </ul>	<ul style="list-style-type: none"> <li>Superhydrophobic, antibacterial and UV-blocking fabric</li> <li>Significant hydrophobicity for 30 s and even after washing</li> </ul>
	Textile dyeing	<ul style="list-style-type: none"> <li>Carnauba Palm (<i>Copernicia Prunifera</i>)</li> <li>Prodigiosin<sup>86,87</sup></li> </ul>	<ul style="list-style-type: none"> <li>Water repellent nano-coating on cotton, nylon and cotton-nylon fabrics<sup>85</sup></li> <li>Production of a pyrrole structure pigment by cell metabolism<sup>88</sup></li> </ul>	<ul style="list-style-type: none"> <li>Environment friendly water repellent textiles exhibiting good air permeability and antibacterial effect</li> <li>Better mass transfer rate for positively charged substances</li> </ul>

of nanotechnology that encompasses different areas of the field in a single study. With that inspiration, in this work, we will review various applications, advancements, and advantages of biomimicry in the field of nanotechnology.

A comprehensive overview of this review paper is given in Table 1, which summarizes the application of biomimicry in various fields of nanotechnology.

## 2 Biomimicry and nanosensors

Nanosensors are nano-devices used for sensing physical, real-life quantities that can later be converted into detectable signals. Although nanosensors are used in a variety of domains, they have a similar workflow: (i) binding, (ii) signal generation, and (iii) processing. Major advantages of using nanosensors (compared to their macro counterpart) are increased sensitivity and specificity, lower cost, and better response times. Taking inspiration from mother nature, researchers and scientists are now trying to design nanosensors that very closely emulate nature's sophisticated way of effortlessly binding to an analyte or generating signals. While there are many studies that review nanosensors in light of specific applications,<sup>89-92</sup> there still ceases to exist any comprehensive review on "biomimicry and nanosensors". In this section, we will review some of the nanosensors which were designed by taking inspirations from the biosphere, specifically in the following domains: optical nanosensing, peptide nanosensing, tactile nanosensing, and stimuli responsive nanosensing (Fig. 1).

### 2.1 Biomimetic optical nanosensors

Research in the field of nanosensors has paved the way for the successful implementation of chemical, infrared and

mechanical sensors, all of which have vast applications in modern-day technology, from tensile strength of wires to the design of an aerospace vehicle.<sup>97</sup>

Many biological creatures have "built-in" infrared (IR) sensing capabilities. Emulating this particular characteristic has led to the fabrication of a biomimetic IR receptor micro-sensor. Some families of pythons, boas, and even beetles have infrared sensing organs, which sometimes convert IR radiation into heat, which in turn results in a thermal-sensitive system. In the inspired sensor, the incident IR radiation warms a liquid, thus inducing a mechanical deformation of the membrane, which is spotted in a capacitor.<sup>98</sup> This is possible because temperature changes can be detected by closely monitoring the changes in the capacitance. The main advantage of such a sensor is that it can be used at room temperature without any additional active cooling, unlike other photo detectors.

Recently, another optical sensor that is aided by the common housefly has been developed which can be used for aircraft wing deflection. The functionality of a compound eye is the wider field-of-view detection and other image processing techniques. The advantage of such a sensor is its low weight, less power consumption, faster computation, and better form factor.

Many animals use their ability to change their coloration for communication, predator capturing, camouflage, etc. This ability to change color has pushed engineers to make sensors that change color in the presence of certain chemicals, hence acting as a chemical sensing sensor. The iridescent scales of some butterflies also show variation in their optical properties when exposed to different kinds of vapors.<sup>99</sup> These phenomena of the natural system aided researchers to build photonic vapor sensors. Another device which consisted of periodic ridges and lamella deposited on a silicon wafer showed strong reflectance



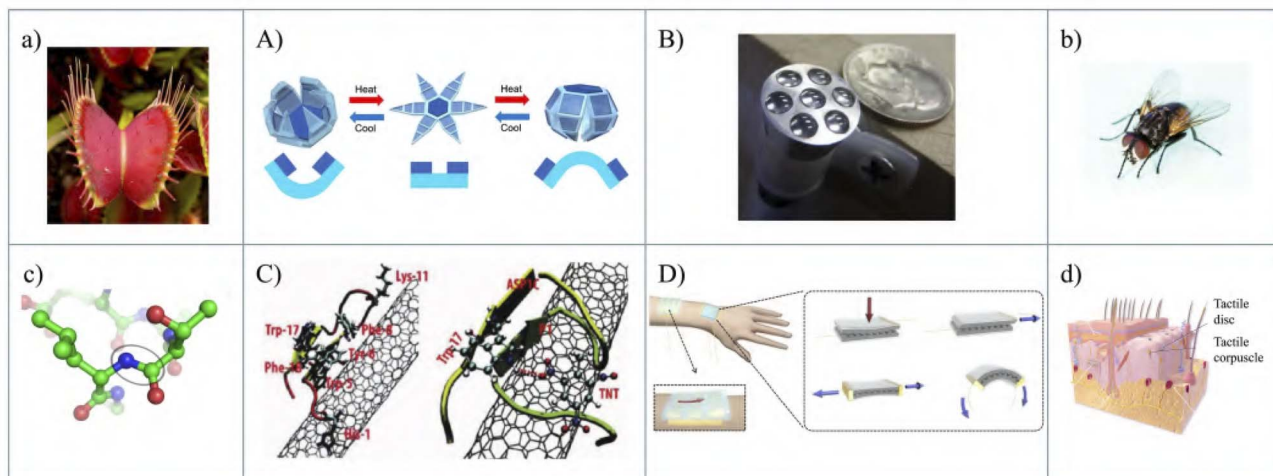


**Fig. 1** Biomimicry in nanosensors.\* (a) Venus flytrap [self-published photograph<sup>93</sup>]. (A) Thermo-responsive self-folding microgrippers [inspired by (a)]. Figure reproduced from ref. 31 with permission from the American Chemical Society, copyright 2015]. (b) Common housefly [self-published photograph<sup>94</sup>]. (B) Aircraft wing deflection sensor [inspired by (b)]. Figure reproduced from ref. 25 with permission from the American Institute of Aeronautics and Astronautics, Inc., copyright 2015]. (c) Peptide bonds [self-published photograph<sup>95</sup>]. (C) Nano-electronic noses [inspired by (c)]. Figure reproduced from ref. 29 with permission from the American Chemical Society, copyright 2012]. (d) Human skin mechanoreceptors [self-published work<sup>96</sup>]. (D) Skin-attachable adhesives (E-skins) [inspired by (d)]. Figure reproduced from ref. 30 with permission from the American Chemical Society, copyright 2014]. \*In this article, when we present natural inspiration and the corresponding technology that it led to in the same figure, we use a lowercase English letter for the inspiration and the corresponding uppercase English letter for the technology. For example, (a) inspires (A).

in well-defined spectral regions. These are some of the prime examples of how researchers, scientists and engineers have mimicked Mother Nature's light exploitation techniques to fabricate optical nanosensors.

## 2.2 Biomimetic peptide nanosensors

By coupling peptides to a common nanomaterial surface (graphene and carbon nanotubes) a peptide nanosensor is created, which is capable of distinguishing chemically camouflaged mixtures of vapors and detecting chemical warfare agents at a parts-per-billion level.<sup>29</sup>

## 2.3 Biomimetic tactile nanosensors

Tactile wearable sensors that can receive information upon physical contact have gained a lot of attention from researchers and have potential usage in healthcare, robotic, and wearable device applications. Researchers are now working on tactile nanosensors that are based on biological tactile systems.<sup>100</sup> The main challenge of such a device is mimicking the human skin mechanoreceptors-receiving and transducing physical stimuli to electrical signals *i.e.* action potentials, and the biomimetic signal processing mechanism.<sup>101</sup>

## 2.4 Biomimetic stimuli responsive grippers

Inspired by the Venus flytrap, many stimuli-responsive, biomimetic shape-changing robots/actuators have been proposed by combining stimuli-responsive hydrogels, polymers, or their hybrid combination.<sup>32</sup> These grippers actually have far-reaching

applications in the fields of biosensors, smart medicine, robotics, and surgery. Hydrogels and polymers are best suited for this purpose because they have the same moduli ranges ( $\sim$ kPa) of biological tissues and they can extend up to several orders of magnitude in volume when perturbed with external stimuli. This extending and shrinking mechanism replicates the self-actuating action without any external electrical power sources. The main material for this type of gripper is *N*-isopropylacrylamide (NIPAM) based stimuli-responsive hydrogels, and liquid crystalline material-based stimuli-responsive hydrogels.

## 3 Biomimicry in nanomedicine

Biomimicry means technological achievements that have been developed using inspiration found in nature. The application of nanotechnology in healthcare is referred to as nanomedicine, and biomimicry is the inspiration for it because the human body is a gift of nature and riddled with questions and answers. In the sense of understanding natural structures and using this knowledge to perform and develop many tasks, nanomedicine may be regarded as a specialized division of biomimicry. Biomimicry assists in bone regeneration by use of self-assembled nanostructure tissues,<sup>33</sup> hydrogels<sup>38–40,102</sup> or electrospinning.<sup>103</sup> Skin<sup>104,105</sup> and nerve restoration are another important aspect of biomimicry application in nanomedicine.<sup>106</sup> Biomimetic nanorobots are another application of biomimicry in nanomedicine. Inspired by platelets<sup>107,108</sup> and platelet-membrane-cloaked



nanomotors, they perform the task of adsorption and isolation of platelet-targeting biological agents.<sup>109</sup>

### 3.1 Tissue engineering and surgery

Plastic surgery is used to reconstruct tissues lost due to injury, but it has evolved so much from the surgical practice of 30 years ago. Previously, doctors used synthetic implants using silicone,<sup>110</sup> cellulose,<sup>111</sup> etc. but they might interact with the host in a harmful manner, resulting in infection and rare tumors. And those implants did not replicate biological tissues. Vascularized composite tissue allotransplantation (VCA) was the first reconstructive milestone, but it had inevitable probabilities like transplant rejection. Tissue engineering then became the best alternative solution since this process does not have those limitations.<sup>41</sup> Research on self-assembling biomaterials that mimic complex biological structures has also been going on for a long time. Molecules that self-assemble into a nanostructured gel, replicate the key characteristics of the human bone extracellular matrix (ECM). This is extremely important for the generation of bony tissues.<sup>33</sup>

Biomimetic materials also support a microenvironment for cell attachment, proliferation, differentiation, and ultimately tissue regeneration. For example, the most abundant ECM protein in our body is collagen.<sup>112</sup> A number of natural micro-molecules (collagen,<sup>34</sup> silk fibrin,<sup>35</sup> fibrinogen, synthetic polymers (poly[glycolic acid],<sup>36</sup> poly[L-lactic acid],<sup>37</sup> and poly[lactic-co-glycolic acid]) have been processed using electrospinning. This technique builds scaffolds that mimic natural tissues. To produce good scaffolds the biomaterial has to be both biocompatible and support cell growth. This will allow the scaffold to continue the metabolic functions. Moreover, it must promote integration with host tissue and allow vascularization.<sup>103</sup>

Since the early 90s, multiple biomaterials have been exploited for cartilage and bone applications. And recently, hydrogels have become popular due to their network of interacting hydrophilic polymer chains that have striking similarities with a native tissue ECM.<sup>38</sup> Hydrogels maintain the cell structure<sup>39</sup> and provide strong mechanical support.<sup>40</sup> In the case of bone repair, hydrogels bond with the natural ECM strongly.<sup>102</sup> And hydrosols can be injected at the injury site, and they adjust themselves to match the shape of the injury.<sup>38</sup> Artificial bone substitutes have been produced from mineral compositions, ceramic or material, bioglass, or other fiber materials to replicate the organic tissue fraction as boney tissues.<sup>113</sup> However, due to the inability to fully master the level of growing fully functional bone with cortical bone components, bone replacement surgical techniques such as non-vascularized or vascularized bone transfer or the Masquelet technique to support bone construction by maintaining flap coverage are used.<sup>113-115</sup>

Skin is also an important part of the human body that can receive damage from various sources, such as burns and infections. When a skin defect reaches the deep dermal layer, the self-regeneration potential of the skin is obstructed, and artificial skin substitutes using biomimicry can assist in skin repair.<sup>105</sup> Artificial skin substitutes have been constructed with different compositions and material properties, mimicking the

organization of normal skin.<sup>116</sup> Examples are the collagen matrix bonded to a flexible nylon fabric/silicone rubber epidermis<sup>116</sup> or collagen-elastin matrix.<sup>104</sup> Biomimetic scaffolds can also be used for nerve replacement by mimicking the inner structure and surface structure of original nerves.<sup>106</sup>

### 3.2 Biomimetic nanorobots in medical science

One exciting current application of biomimicry is the development of biomimetic nanorobots. These are micro-nanoscale robots for biomedical operations. Industrial robots are used mainly for the automation of dangerous tasks, but biomedical nanorobots are designed to tackle biological events. Biomimetic nanorobot design has recently started to take inspiration from nature, especially from circulating cells such as platelets and leukocytes. Human platelets become the main source of inspiration owing to their work in tackling immune evasion,<sup>107,108</sup> pathogen interactions, and hemostasis. The platelet membrane cloaking method is the wrapping of natural platelet cell membranes onto the surface of nanostructures and nanodevices.<sup>117</sup> These platelet-membrane-cloaked nanomotors are enclosed by human platelets and perform the adsorption and isolation of platelet-targeted biological agents.<sup>109</sup> These PL-motors possess a membrane coating containing multiple functional proteins related to platelets. These PL-motors evade the body's immune system and display rapid locomotion in whole blood. PL-motors can also effectively absorb Shiga toxin using a Vero cell assay and also show binding to pathogens that can be used for rapid bacterial isolation.<sup>109</sup>

Minimally invasive surgery (MIS) and natural orifice trans-luminal endoscopic surgery (NOTES) is gradually taking the place of open surgery as this will decrease patient trauma and recovery length. Viewing the inside of a patient's lumen is a must for MIS. And now soft endoscopic nanorobots, aided by nature, are being used for reaching distant surgical targets. Robot bodies are composed of soft materials that will reduce the potential of damage to tissue or organs. They are also bendable and flexible enough to move inside the patient's lumen. The meshworm design developed by Bernth *et al.* was inspired by the earthworm.<sup>118</sup> The robot is made up of three segments of a soft plastic-silicone mesh composite. The total length of all segments is 50 cm and each segment is actuated by tendon wound mounted on DC motors, which are small enough to be embedded inside biomimetic meshworms. A PID controller controls the length of each tendon, and a USB camera is mounted at the tip (Fig. 2).

Then there can be nanorobots that have hybrid cell membranes – a combination of red blood cell (RBC) and platelet (PL) membranes. This shows better binding than PL-motors and neutralization of PL-adhering pathogens (*Staphylococcus aureus* bacteria) and neutralization of pore-forming toxins ( $\alpha$ -toxin).<sup>119</sup> Some drugs can be carried by platelets because of the site-specific adhesion of platelets. PL – motors can also be used for this purpose.<sup>120</sup>

### 3.3 Nanoparticles

Nanoparticles (NPs) are usually defined as particles having a diameter of between 11 and 100 nm. Nanoparticles have



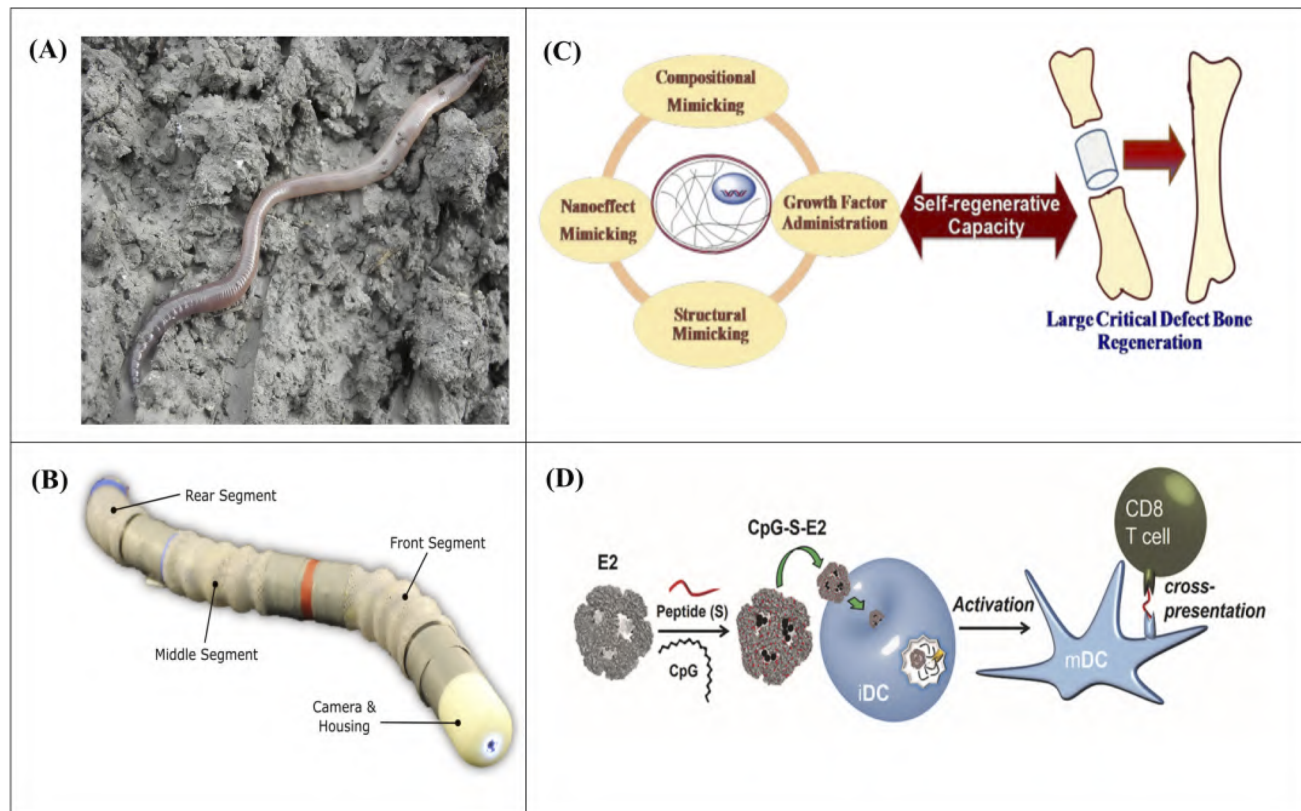


**Fig. 2** Biomimicry in nanomedicine. (A) Earthworm [self-published photograph<sup>121</sup>]. (B) A meshworm equipped with an endoscopic camera [inspired by (A)]. Figure reproduced from ref. 118. (C) schematic diagram of how a combination of nanoelements and growth factor administration may allow regeneration of large critical defect bone. [Figure reproduced from ref. 122 and 123 with permission from the Royal Society of Chemistry, copyright 2017]. (D) Encapsulation of internal influenza proteins on the virus-like-particles (VLPs). [Figure reproduced from ref. 42 with permission from the American Chemical Society, copyright 2013].

unique material characteristics owing to their submicroscopic size. For example, these nanoparticles can be used to improve the activity of different medicines. Many cancer vaccines suffer from the inability to mount a T-cell response. But viruses possess this size, and the immune system can recognize these physical properties. So, replicating these properties with nanoparticles provides a better platform for vaccine design. A viral mimicking vaccine platform capable of encapsulating dendritic cells showed a threefold better reaction than normal cases.<sup>42</sup> A controlled immune response towards a specific virus-cell is also possible, which results in a vaccine that is active against the specific virus at a greater rate. Encapsulation of internal influenza proteins on the interior of virus-like particles (VLPs) results in a vaccine that provides protection against 100 100 times the lethal dose of an influenza.<sup>43</sup> Protein-based nanocages are also of particular interest to researchers because of their excellent ability to deliver drugs to specific sites in the human body. A protein cage nanoparticle, encapsulin, isolated from *Thermotoga Maritima*, has been developed for multifunctional delivery nanoplatforms for both chemical and genetic engineering<sup>44</sup>.

Nanoparticles increase the bioavailability of compounds *via* their large surface-to-volume ratio. Many different nanoparticle systems have been created over the years to influence wound care in the medicine industry. Nanoparticles' responses depend

on external stimuli such as temperature, pH, ultrasound, light, *etc.* Dual emission responses of PL polymeric hydrogel Eu-doped PS-co-PNIPAM/d-TPE-doped PNIPAM-co-PAA nanoparticles are controlled strongly and independently by temperature and pH. These different emission colors can be utilized to distinguish cancer cells from normal cells.<sup>124</sup> pH and temperature variation of the wound help a hydrogel, which is prepared by cross-linking *N*-isopropylacrylamide with acrylic acid and silver nanoparticles (AgNPs) to eliminate 95% of pathogens between pH 7.4 and 10.<sup>125</sup> Ultrasound, which is another stimulus, can disrupt ionically cross-linked hydrogels which can be used to enhance the toxicity of mitoxantrone toward breast cancer cells.<sup>126</sup> Similarly, ultrasound can be used as a trigger to release drugs at specific locations,<sup>127,128</sup> and the length and intensity of the ultrasound pulse can be used to control the amount of drugs used.<sup>129</sup> Upon exposure to either one- or two-photon excitation, a mesoporous silica nanoparticle (MSN) based drug delivery system (DDS) for controlled anticancer drug release was disclosed.<sup>130</sup> In this method, the MSN served as a "photo trigger" for drug release. The precise timing of the anticancer drug's release can be controlled by external light manipulations like varying the irradiation wavelength, intensity, and time. Degradable nanoparticles such as polymeric NPs accelerate wound healing by controlling inflammation, and



fibroblast, and osteoclast activity,<sup>131</sup> and they can also be used as antibacterial agents and stem cells.<sup>132</sup>

## 4 Biomimicry and nanorobots

The recent research explosion in nanotech, with the new discoveries in the bio-molecular field, has brought about a new era in nanorobotics. Nanorobots of any nanostructure can currently handle the task of actuation, intelligence, information processing, sensing, *etc.* at the nano-scale. Some of the important functionalities of a nanorobot are (i) decentralized intelligence or “swarm intelligence” (ii) self-assembly and replication at the nano-scale (iii) signal processing at the nano-scale and (iv) nano to macro interface architecture.<sup>133</sup> In this section, we review some of the recent approaches in this field.

### 4.1 Biomimetic bacteria inspired nanorobots

Wireless nanorobots have had far-reaching biomedical applications. But so far most of the micro/nano swimmers have been imitating the rotary motion of helical bacteria flagella for propulsion, while none of them have the ability to reform themselves in the presence of different external stimuli. Recently, magnetic actuation of self-assembled flagellar nanorobotic swimmers has been discovered.<sup>136</sup>

### 4.2 Biomimetic platelet-camouflaged nanorobots

While the main purpose of the industrial and life-sized robots is to work in a controlled manner and perform some pre-determined tasks that are set beforehand, the task of biomedical nanorobots is to handle different biological environments, and adapt and improvise to the situation. In 2017, a study was published on a biologically interfaced nanorobot, which is made of magnetic helical nanomotors and is cloaked with the plasma membrane of human platelets.<sup>109</sup> This kind of nanorobot shows platelet imitating properties, like binding to toxins or special kinds of pathogens.

A different but kind of similar study in 2018, reported the design, construction, and evaluation of a dual-cell membrane

functionalized nanorobot for the removal of biological threat agents.<sup>46</sup> In this study, the nanorobots consisted of gold nanowires and are camouflaged in hybrid RBC and platelet membranes. This kind of nanorobots can fight against biological threats with no apparent biofouling, while imitating natural cells. In Fig. 3, the preparation and characterization of such a nanorobot are shown.

## 5 Biomimicry and nano energy harvesting technology

The population of our beautiful world is expected to increase to 9 billion by 2050.<sup>137</sup> This will result in an increase in the global energy consumption rate of 40.8 TW in 2050.<sup>138</sup> And the primary means of satisfying this enormous demand (around 80%) is through fossil fuels.<sup>139,140</sup> But fossil fuels are detrimental to both human health and the environment. Burning fossil fuels releases mercury, sulfur dioxide, carbon monoxide, nitrogen oxide and other dangerous pollutants that can cause cancer, blood disorders and respiratory conditions.<sup>141,142</sup> Groundwater and streams are also at risk from the increased use of fossil fuels.<sup>143</sup> Oil spills can endanger aquatic ecosystems and contaminate supplies of drinking water.<sup>144</sup> Fossil fuel extraction and processing significantly degrade the environment and ecosystem as well.<sup>145–147</sup> Furthermore, the amount of remaining fossil fuels are depleting at an alarming rate with the increasing usage<sup>148</sup> leading to the dire need for new alternative energy sources. Renewable energy sources such as solar, wind and wave energy can play a significant role as a replacement for fossil fuels. Nature provides numerous instances of harnessing energy efficiently from these renewable sources. Plants can convert solar energy into simple sugars through the process of photosynthesis. Biological cells can also be an inspiration for energy generation. Different types of biological skin textures can aid in enhancing the absorption ability of solar cells and the movement of kelp can be an inspiration for triboelectric nanogenerators for harnessing ocean energy.<sup>52,53,55–60,149–152</sup> All of these alternative energy-generating and harnessing sources

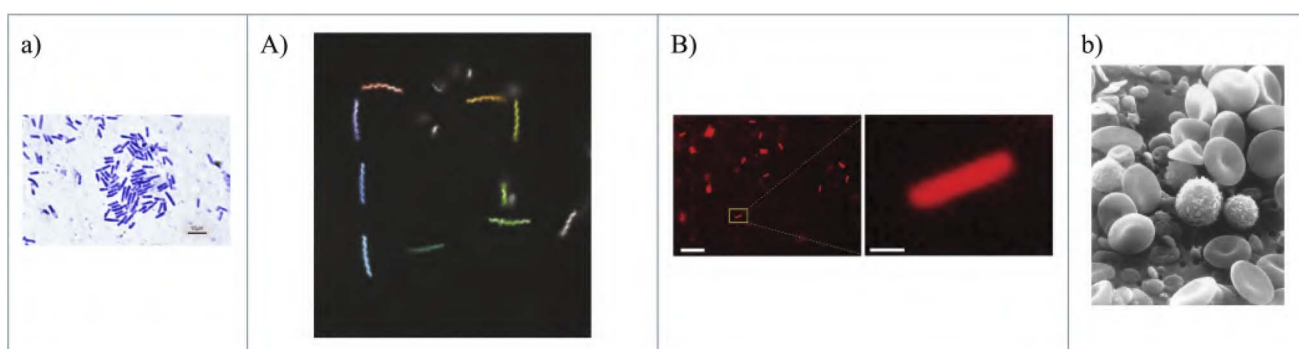


Fig. 3 Biomimicry in nanorobots. (a) *Bacillus subtilis*, a Gram-positive bacterium [self-published work<sup>134</sup>]. (A) Bacteria inspired flagellar curly swimmer nanorobot [inspired by (a). Figure reproduced from ref. 45 with permission from The Author(s), copyright 2017]. (b) SEM image from normal circulating human blood showing red blood cells, several white blood cells, and many small disc-shaped platelets [figure reproduced from ref. 135]. (B) Fluorescent images of PL-motors covered with rhodamine-labeled platelet membranes. Scale bars, 20  $\mu$ m (left) and 1  $\mu$ m (right) [inspired by (b). Figure reproduced from ref. 47 with permission from WILEY-VCH Verlag GmbH & Co., copyright 2017].



aided by nature will greatly assist in meeting the huge energy demand of the future.

### 5.1 Solar energy

Energy is a must for humankind. The current focus of the world is on non-polluting sources of energy, and solar energy is the most desirable of them. 98% of photovoltaic cells are silicon based<sup>153</sup> but solar cells require 99.999% pure silicon, which is very energy intensive and whose production steps also create hazardous byproducts.

Biomimicry is now being used to harvest solar energy from sunlight. The photosynthesis process used by plants leaves no waste. So the inspiration is there to use biomimicry in a solar cell. One such cell is the Gratzel cell<sup>49</sup> in which Gratzel used anthocyanin to recreate photosynthesis. This cell does not use silicon or other heavy metals, and this is much greener for the environment. The downside is that they are not as efficient as silicon cells.

A Gratzel solar cell (also known as a dye-sensitized solar cell or DSSC) mimics the photosynthetic system by having titanium dioxide ( $TiO_2$ ) as  $NADP^+$  and carbon dioxide, iodide as a water molecule, and triiodide as oxygen. They harvest the solar energy together in nano-scale systems.<sup>49</sup> A basic DSC cell has an energy conversion efficiency of 1% under direct radiation. But using thymol, which has 10% of the mass of the dye from cyanin 3-glucoside and cyanin 3-rutinoside, improved the efficiency.<sup>154</sup> The efficiency of DSSCs has exceeded 12% after the last twenty years of development. The amount of light absorbed within the dye is an important part of determining efficiency. For this reason, suitable structures can improve the power conversion efficiency further.<sup>155,156</sup>

Another approach to improving the efficiency of DSC cells has been the modification and optimization of titania photo-electrodes. One approach was to use sphere voids and large-sized solid particles as a scattering center<sup>149,150</sup> or use a multilayer structure<sup>151</sup> on the surface of the photoanode. These steps resulted in an increase in the optical path length of the photo-anode and a subsequent increase in the light absorption efficiency. Another option is to use new structural materials that can increase the optical path length *via* light trapping. Butterfly wings have microstructures that are effective solar collectors or blocks. Solar heat is absorbed at a faster rate at the ribs in the wing, which increases the body temperature faster. Then scientists discovered that honeycomb structures are less reactive than cross-ribbing structures, and that this structure also has a greater advantage in terms of light trapping. Scales have a high refractive index, and so total internal reflection occurs more, and nearly all incident light is absorbed. So, inspired by this, a butterfly wing-scale titania film photoanode improved the light absorptivity of the DSC photoanode.<sup>52</sup> This structure showed perfect light absorptivity and a higher surface area. This increased the total light harvesting efficiency and dye absorption.

Bioreplication has also become recently popular due to its application in solar energy harvesting. Its application in solar energy is based on two observations, the first observation is the wide angular field that many insects, such as flies have. Each eye

of a fly is a compound eye, consisting of multiple elementary eyes. These are arranged radially on a curved surface. The second observation is the almost halving of the reflectance, which is calculated by using a simulation of a prismatic compound lens adhering to a silicon solar cell.<sup>53</sup>

This experimental technique called the Nano4Bio technique<sup>54</sup> has been designed to replicate the layer of a compound eye from an actual specimen. The idea is that by covering the surface of a solar cell with numerous replicas, the angular field of view of the solar cell will increase. The Nano4bio technique can produce multiple replicas simultaneously of multiple biotemplates.

Solar cell efficiency is mainly bound by light-harvesting efficiency, and some research is being done to use the photosynthetic leaf structures to increase the solar cell efficiency. Using a nano-structured poly-carbonate thin-film inspired by the leaves of *Salvinia cucullata* and *Pistia stratiotes* helped design a crystalline Si semiconductor with 18.1% power conversion efficiency (PCE).<sup>157</sup> The light-trapping coating inspired by the epidermal cells in leaves helped in the fabrication of a graphene/Si Schottky junction.<sup>158</sup> The leaf anatomy combined the upper and lower epidermis, palisade, and spongy mesophylls. This upper epidermal layer increases the path length and allows light to traverse deep into the leaf. The middle layer has spongy mesophylls that scatter the light, and this scattered light has a higher chance of absorption by the lower part of the chlorophylls.

### 5.2 Ocean energy

Ocean waves are a great source of renewable energy as they cover almost 70% of the earth. But unlike solar and wind energy, ocean wave energy harnessing techniques have not developed so much yet.<sup>159–161</sup> The integration of offshore wind power plants with ocean wave energy technology could enable power generation in a low-cost and more efficient way, which is obstructed by the deficit of mature wave energy harvesting technology.<sup>162,163</sup>

To collect energy from wave energy, inspiration from kelp, a marine seaweed, has enabled the design of a triboelectric nanogenerator (TENG). Using a conjunction of triboelectric and electrostatic induction effects, a TNG can convert mechanical energy into electrical energy.<sup>55–59,152</sup> A kelp-inspired TENG is made of vertically free-standing polymer strips which could sway independently to cause a contact separation with the neighboring strips, with the vibration of a TENG in water mimicking the gentle sway of kelp. A single unit of a BITENG (bio-inspired TENG) provides an output short circuit current of about 10  $\mu A$  and an open circuit voltage of 260 volts with a maximum power density of 25  $\mu W\ cm^{-2}$  which is high enough to drive 60 LEDs.<sup>60</sup> A network of BITENGs can collect more energy from ocean waves and be integrated with an offshore windmill for generating electricity.

### 5.3 Nanoleaves and nano trees

Another emerging application of biomimicry in the field of energy harvesting is nanoleaves and stems of artificially created



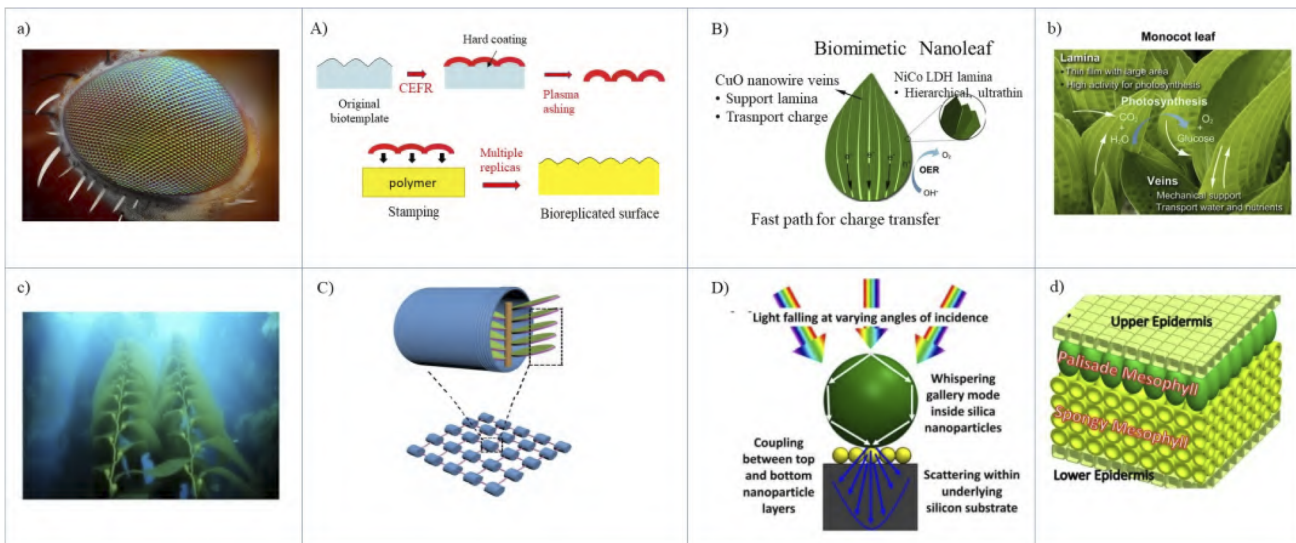


**Fig. 4** Biomimicry in nanoenergy harvest. (a) Compound eye of fly [self-published photograph<sup>167</sup>]. (A) Nano4Bio technique developed to replicate the corneal layer of a compound eye from an actual specimen recreated from ref. 54 [inspired by (a)]. (B) Photograph of a monocot leaf [figure reproduced from ref. 48 with permission from Elsevier, copyright 2019]. (B) Biomimetic nanoleaf<sup>48</sup> [inspired by (b)]. Figure reproduced from ref. 48 with permission from Elsevier, copyright 2019]. (C) Images of a kelp plant [figure reproduced from ref. 60 with permission from Elsevier, copyright 2019]. (C) Schematic diagrams of a TENG-unit, the kelp-inspired TENG design and the networks [inspired by (c)]. Figure reproduced from ref. 60 with permission from Elsevier, copyright 2019]. (d) Schematic of leaf anatomy which inspired the light-trapping coating [figure reproduced from ref. 158 with permission from Elsevier, copyright 2019]. (D) Light management mechanism in a bilayer light-trapping scheme with an all-dielectric sphere. [inspired by (d)]. Figure reproduced from ref. 158 with permission from Elsevier, copyright 2019].

trees or plants.<sup>51</sup> The nanoleaves are distributed throughout artificial trees and plants, and they can supply a whole household's electricity demand under optimum conditions.<sup>164,165</sup> A nanoleaf has two sides, one side has a very thin photovoltaic film that converts the light from the sun into energy. On the other hand, thin thermo-voltaic films convert heat from solar energy into electricity.<sup>50</sup> So, the sunlight is then converted into electricity when it falls onto the nanoleaves.

Inspired by the leaf structure in nature, a biomimetic nanoleaf was developed for the first time.<sup>48</sup> The fabricated nanoleaves contain a thin lamina and parallel veins, forming a monocot leaf structure. CuO nanowires with a high density on a conductive Cu mesh were used as the veins to support the layered double hydroxide (LDH) nanosheet lamina and promote charge transfer. Using CuO/GNS composites with microwave assistance is another quick, time-saving, and environmentally responsible way to make nanoleaves. Due to the strong coordination between graphene and CuO, this performs better than pristine CuO nanoleaves<sup>166</sup> (Fig. 4).

## 6 Biomimetic nanostructures and photonics

Over the years, nature, through evolution, has aided photonics researchers by providing a great variety of biological nanostructures. This has enabled them to design new devices and modify the existing ones to enhance performance. Prevalent biological photonic structures are developed and optimized to perform necessary tasks for that creature, such as camouflage,

courtship, warning or attraction to conspecifics, pollination, and so on.<sup>173–175</sup> Structural coloration and iridescence of insects, birds' feathers, plants,<sup>174,176–179</sup> densely arrayed triangular hairs on Saharan ants for thermoregulation<sup>180</sup>, anti-reflecting coating of moth and butterfly eyes<sup>181,182</sup> and on the transparent wings of hawkmoth,<sup>183</sup> the apparent 'metallic' view of a fish scale<sup>173</sup> etc. are the instances of photonic structures existing in nature. In this section, we will review the applications of such natural structures in the area of nanophotonics. Mainly we will review how biomimetic structures can improve the absorption, reflectance, and transmittance spectra. Fig. 5 summarizes the applications of a few such biomimetic structures in nanophotonics.

In 1967, Bernhard discovered that the reflection over the visible range (400 to 800 nm) from the corneas of night flying moths is reduced because of their having tiny conical burls.<sup>184,185</sup> This has led to the discovery of an artificial moth eye, which is a very fine array of protuberances. The working of an artificial moth-eye surface may be understood with the help of the surface layer, which has a gradually changing refractive index having a value from unity to that of the bulk. Due to the presence of gradually varying refractive index layers, the net reflectance is the resultant of an infinite series of reflections at each incremental change in the index. Each of these reflections has different phase factors because of the change in the depth of different layers. Now if this occurs over a distance of  $\frac{\lambda}{2}$ , all the phases will be present, which will result in destructive interference and so the net reflectance will be zero.



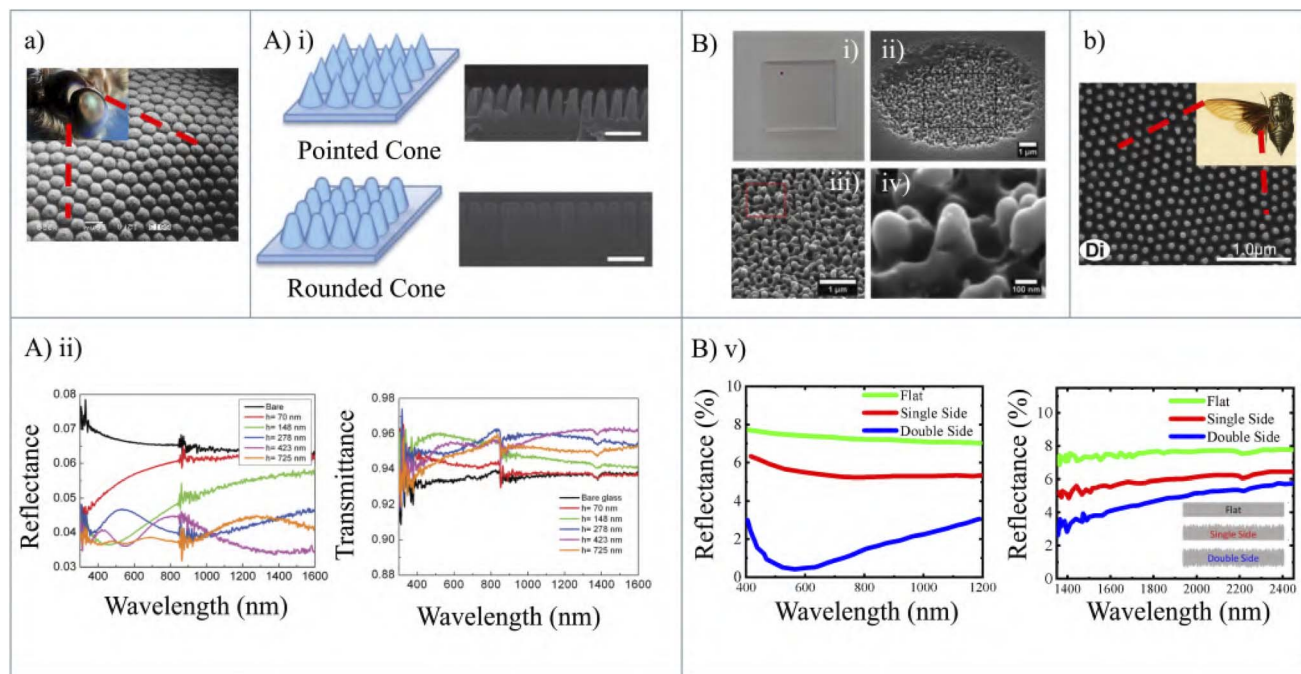


**Fig. 5** Biomimetic structures in nanophotonics. (a) Actual and SEM images of the eyes of a moth [self-published work<sup>168,169</sup>]. (A) (i) Moth eye inspired anti-reflective nanocones. The upper one is a pointed cone and its SEM image. The lower one is a rounded cone and its SEM image. The scale bars in the SEM images are all 500 nm (ii) measured reflectance and transmittance of the moth eye inspired nanocones and the bare structures [both inspired by (a)]. Figure reproduced from ref. 170 with permission from The RSC Pub, copyright 2012]. (b) SEM image of *Cryptotympana atrata* (cicada species) wing surfaces [(inset) self-published work,<sup>171</sup> figure reproduced from ref. 172 with permission from PLoS One]. (B) (i-iv) Photographs and SEM image of an omnidirectional anti-reflective glass inspired from a Cicada Cretensis scale [inspired by (b)]. (v) Reflectance spectra of a pristine (green lines) and laser-treated at one (red lines) or both side (blue lines) fused silica plate. Reflectance in both cases decreases with the introduction of a biomimetic anti-reflection coating [all inspired by (b)]. Figure reproduced from ref. 78 with permission from The WILEY-VCH Verlag GmbH & Co., copyright 2019].

## 6.1 Moth-eye nanostructures

The spacing of the protuberances of the moth-eye must be small enough that the array cannot be resolved by the incident light; otherwise, the array will work as a diffraction grating and the light will simply be redistributed into the diffracted orders.<sup>181</sup> The optical properties of an artificial moth-eye surface depend on the height of the protuberances and their spacing. The pattern of the moth-eye array is a photo-resist interference fringe at the intersection of two coherent laser beams.<sup>185</sup> The advantage of moth eye anti-reflection coating applied to a high-quality optical component comes at larger angles of incidence. In the case of normal incidence, the moth-eye has the same performance as conventional multilayer coating techniques. But at a larger angle of incidence, the performance of the former is better than that of the latter. In a work presented in 2013, a group showed a comparative study of three different anti-reflecting structures (ARSs) for broadband and angle-independent anti-reflection,<sup>61</sup> both theoretically and experimentally. These structures were single diameter nanorods (ARS I), dual diameter nanorods (ARS II), and biomimetic nanotips (ARS III) which take after the submicron structure of a moth's eyes. The simulations were performed using finite difference time domain calculations. All the structures were made of Si. The structures along with the refractive index profile are shown in Fig. 6(a) and (b).

The three structures, along with a planar Si wafer (used as a reference) were simulated using FDTD to obtain the results of reflectance and absorption over 250–1100 nm. Fig. 6(c) shows the resulting reflectance and absorption over the mentioned wavelength region. From Fig. 6(c) it is seen that ARS-III has the lowest reflectance value among the others and in the case of absorption shown in Fig. 6(b), it has almost 98% absorption over the wavelength range.

The dependence of reflectance on the angle of incidence (AOI) was studied from 5° to 85° using unpolarized, s-polarized, and p-polarized light with a wavelength of 633 nm. It is seen from Fig. 6(d) that irrespective of polarization, the reflectance of the ARS III structure shows almost no AOI dependence below the Brewster angle (~75°). From these results, it is concluded that ARS III inspired by the structure of moth eyes, has shown better performance as an anti-reflector than both ARS I and ARS II.

In the case of a solar cell, the greater the absorption of the incident light, the greater the efficiency. So a moth-eye is integrated into solar cells to increase the efficiency of solar cells. As we have seen earlier, a moth-eye anti-reflecting coating has virtually zero dependence of reflectance on the angle of incidence. This property can be exploited in an organic solar cell to enhance performances.<sup>62</sup> Forberich *et al.*<sup>62</sup> fabricated a type of organic solar cell with a moth-eye anti-reflective coating as an

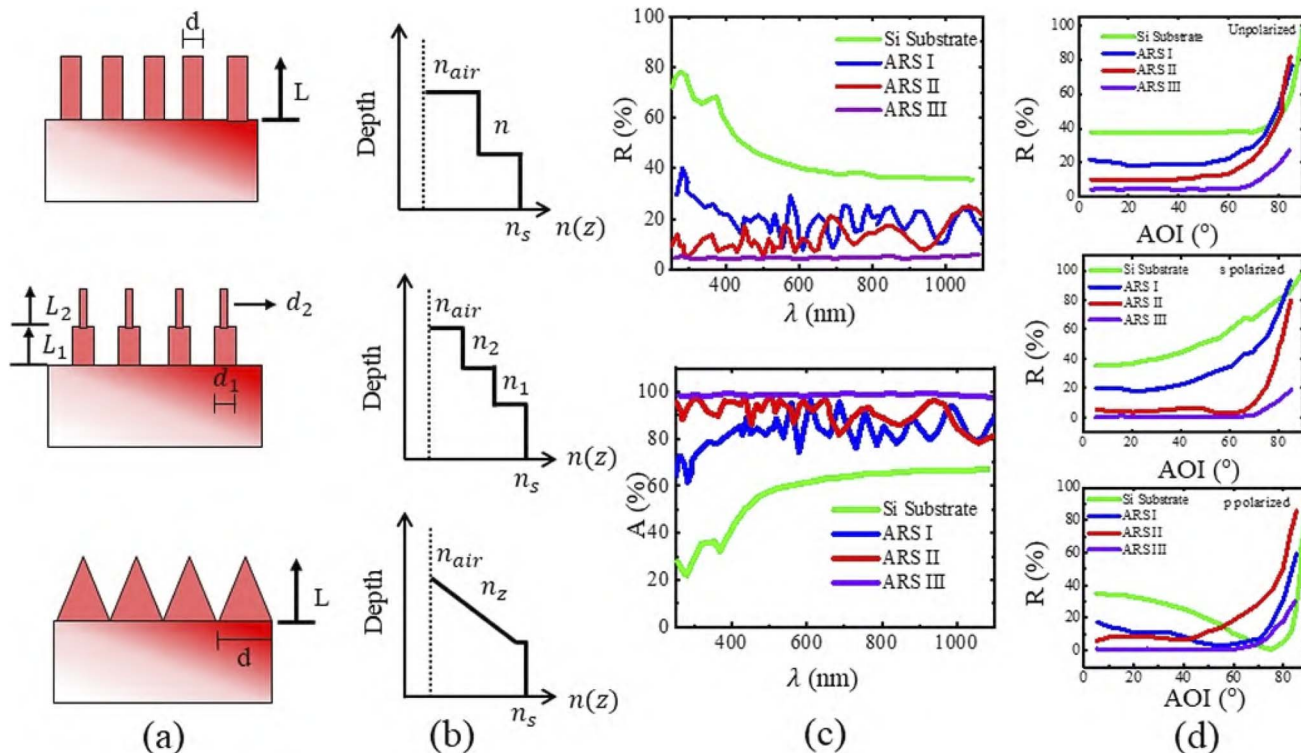


Fig. 6 (a) Schematic diagram of three types of Si ARSSs with the corresponding geometrical parameters. (b) The refractive index profile for each ARS. The refractive index of air, Si and the mixture of air/Si is represented by  $n_{air}$ ,  $n_s$ ,  $n_{1/2}$  respectively.  $n_z$  represents the gradient index of refraction as a function of depth, which is in the  $z$  direction. (c) Reflectance and absorption as a function of wavelength for three types of ARSSs with a reference planar Si substrate. R stands for reflectance and A stands for absorption. (d) Reflectance data for a Si wafer, ARS I, ARS II, ARS III as a function of angle of incidence (AOI) for unpolarized light, s-polarized light, and p-polarized light with a wavelength of 633 nm. The spectrum is almost independent of the incident angle for a biomimetic ARS [figure reproduced from ref. 61 with permission from the Society of Photo-Optical Instrumentation Engineers (SPIE), copyright 2013].

effective medium at the air–substrate interface. The organic solar cell consisted of a thin (~20 nm) layer of poly(3,4-ethylenedioxythiophene) doped with poly(styrene sulfonate) (PEDOT:PSS Baytron, Bayer AG) on indium tin oxide (ITO) coated on a glass substrate. The moth-eye was introduced at the air–glass interface.

The measurement results are shown in Fig. 7(a) and (b). From the reflectance *vs.* wavelength curve for glass/ITO/PEDOT stacks, both curves show oscillatory behavior due to interference in the dielectric slab. However, in the case of moth eye/glass/ITO/PEDOT, the overall reflection is reduced due to the introduction of a moth-eye layer. Fig. 7(b) shows the result of state-of-the-art P3HT:PCBM solar cells with and without moth eyes.

Here it is observed that the highest reduction of reflection occurs in the 350 to 600 nm wavelength range. And beyond that, the reflection becomes almost identical. This happens because, in the case of longer wavelengths, most of the incident light is reflected from the metal electrode, and so the reduction of reflection at the air–glass interface has no significant effect on the overall reflection. From the measured incident angle dependence of external quantum efficiency (EQE) of the P3HT:PCBM solar cell with a moth-eye anti-reflective coating, it

is found that at  $0^\circ$  incidence *i.e.*, normal incident, the EQE increases by around 3.5% with the introduction of moth eyes in a complete solar cell. In fact, EQE is greater with moth eyes than with a normal solar cell for all angles of incidence.

Zhu *et al.*<sup>63</sup> reported a nanocone solar cell. It had efficient optical properties with a great processing advantage over nanowire and thin-film solar cells. The work found that the nanocone arrays had shown absorption above 93% which was

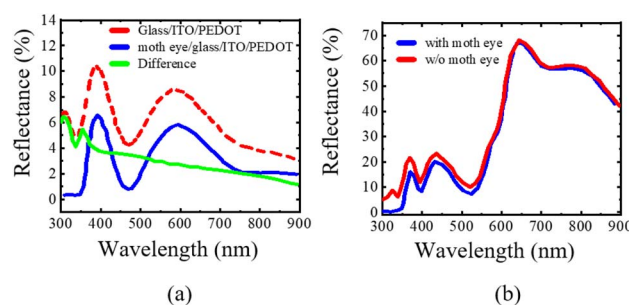


Fig. 7 Measured reflection with and without a moth eye from a layer stack of (a) glass/ITO/PEDOT and (b) a P3HT:PCBM solar cell [figure reproduced from ref. 62 with permission from Elsevier B.V., copyright 2007].



much greater than the nanowire arrays (75%) or thin films (64%) in the wavelength range of 400–600 nm.<sup>64,65</sup>

In another work, biomimetic nanostructured antireflection coatings with polymethyl methacrylate (PMMA) layers were integrated with silicon crystalline solar cells. The structure could reduce the average reflectance of solar cells from 13.2% to 7.8%. As a result, power conversion efficiency increased from 12.85% to 14.2%.<sup>66</sup>

The anti-reflector moth eye used in perovskite solar cells can improve performance significantly. All-inorganic carbon-based perovskite solar cells (PSCs) have drawn increasing interest among researchers due to their low cost and the balance between bandgap and stability.<sup>67</sup> However, due to the reflection at the air/glass interface, such PSCs suffer an optical loss of about 10% of the incident photons.<sup>186,187</sup> This optical loss results in a reduction in the short circuit current density ( $J_{sc}$ ) for PSCs. The inclusion of moth-eye antireflection (AR) nanostructures with wide-range-wavelength AR properties have paved the way to solve the optical loss issue of the above-mentioned PSCs and enhance the power conversion efficiency (PCE).<sup>67–73</sup> Compared to the conventional AR, the additional benefit of moth-eye ARs is the enhancement of broadband antireflection through the tuning of structural and geometrical parameters *i.e.* height, periodic distance, shape, and arrangement.<sup>73</sup> Such modulation of optical properties of moth-eye ARs gives rise to new directions to increase the PCE of PSCs. 300 nm and 1000 nm inverted moth-eye structured polydimethylsiloxane (PDMS) films were fabricated using soft lithography and are reported in ref. 72. The former one abated the optical loss at the air/glass interface and enhanced the solar cell efficiency by about 21% from 19.66% and  $J_{sc}$  from 23.83 mA cm<sup>-2</sup> to 25.11 mA cm<sup>-2</sup>. The 1000 nm moth-eye structured PDMS films exhibit elegant coloration due to the interference originating from the diffraction grating effect. Ormostamp-based moth-eye AR has been fabricated using the nano-imprinting method and included on the glass side of the all-inorganic carbon-based CsPbIBr<sub>2</sub> PSCs in ref. 67. This resulted in an increase of  $J_{sc}$  from 10.89 mA cm<sup>-2</sup> to 11.91 mA cm<sup>-2</sup> and PCE increased from 9.17% to 10.08%. The solar cell also showed excellent adaptability to higher temperatures up to 200°.

A superhydrophobic surface is another application of moth-eye structures apart from the anti-reflection coatings. Moth-eye textured surfaces, due to their roughness, possess enhanced water-repellent properties, resulting in a superhydrophobic surface. Such structures have been utilized to fabricate foldable displays for various electronic devices. The transmission property of the structures remains almost invariant under different bending, thermal, and chemical conditions. Hence, the resulting displays show very good anti-reflective function, excellent mechanical resilience, and foldability, as well as superhydrophobicity with good thermal and chemical resistance.<sup>74</sup>

## 6.2 Anti-reflective transparent nanostructures

*Greta Oto*, commonly known as the glasswing butterfly, and the *cicada Cretensis* species possesses unique transparent wings

with broadband and omnidirectional anti-reflection property. This property originates from the presence of nanopillars having periodicity in the range of 150–250 nm on the wing's surface resulting in a gradient of refractive index between air and the wing's membrane.<sup>75–77</sup> This property aided the fabrication of omnidirectional anti-reflective glass which can show a reflectivity smaller than 1% irrespective of incident angles in the visible spectrum for S-P linearly polarized configurations.<sup>78</sup> Such biomimetic anti-reflective transparent materials have pervasive applications including in displays, solar windows, optical components, and devices.<sup>188–195</sup> A single-step laser texturing approach, and nanosecond, and femtosecond laser processing systems are used to fabricate such anti-reflective transparent structures.<sup>78,196,197</sup>

## 7 Biomimetic nanotechnology in textile engineering

Textiles have been an integral part of human civilization for a long time. Humans started using textiles to protect themselves from the cold and other adverse conditions. With time, the trend and manufacturing process in textiles has changed tremendously. Natural elements showing superhydrophobicity, self-cleaning properties, structural color, and fine quality of fabric have aided textile engineers and researchers to develop more sophisticated textiles with enhanced performances and functionalities. In this section, we will review some of the research work related to nano-biomimicry in the field of textile engineering.

### 7.1 Water repellent textiles

Superhydrophobicity and self-cleaning properties are prevalent in nature in various plants. The most common and notable example is the lotus. Due to the higher contact angle ( $\geq 150^\circ$ ), virtually no wetting of the surface takes place on a superhydrophobic surface, leading to the property of self-cleaning. Whenever rain falls on a lotus leaf, the water droplets roll off as a result of a higher contact angle, and on its way, it collects dirt or other materials, cleaning the surface and keeping the leaves dry and free of pathogens.<sup>79–81,83</sup>

Nanotex was founded in 1998. It was based on the idea of superhydrophobicity *i.e.*, repelling water from a surface. They implemented this natural process using nanotechnology, where nanomolecules bonded to the textiles provided an efficient stain-repellent mechanism. This eventually led to the removal of stains and dirt. This technology is now used in over 100 brands around the world. In another research work published in 2013, the superhydrophobicity of lotus leaves inspired the development of a simple coating method using silver nanoparticles (AgNPs). This could facilitate the bionic creation of superhydrophobic surfaces on cotton textiles with the functionality of water repellency, and antibacterial, and UV blocking.<sup>84</sup> In this work, NaOH-soaked cotton fiber was immersed into the aqueous solution which resulted in the formation of silver cellulosate which finally formed AgNPs through reduction of Ag cellulosate by C<sub>6</sub>H<sub>6</sub>O<sub>8</sub> solution. This Ag-coated cotton



fabric was then immersed into prehydrolyzed OTES (octyl-triethoxsilane) and the final fabric was called “Cot-Ag-OTES”. This fabric was then subjected to ultraviolet-visible reflectance spectrophotometry, scanning electron microscopy, energy dispersive X-ray spectroscopy, and X-ray diffractometry for characterization. The superhydrophobicity was determined by measuring a 5  $\mu\text{L}$  water droplet contact angle (CA) and shedding angle (SHA). Cot-OTES (the sample without AgNPs) had a CA of  $135^\circ \pm 5.2^\circ$  and water SHA of  $31^\circ$ . But with the introduction of a AgNP coating, the CA was found to be  $156^\circ \pm 3.8^\circ$  and SHA,  $8^\circ$ . This proves the performance enhancement of the water repellence properties of the Cot-Ag-OTES sample. Fig. 8(A)(i-iii) show the optical micrographs of 5  $\mu\text{L}$  water droplets on the surfaces of the untreated (i) Cot-OTES (ii) Cot-Ag-OTES and (iii) fabric samples. With the introduction of AgNPs, the increase of contact angle and hence the hydrophobic properties is evident in this figure. SEM micrographs of untreated and AgNP treated cotton samples are given in Fig. 8(A)(iv and v) and (A)(vi and vii), respectively. In 8(A)(vii), the water droplets are visible on the sample, ensuring its hydrophobic properties. Gram-negative *E. coli* and Gram-positive *S. aureus* bacteria were used to evaluate the anti-bacterial properties of the samples. It turned out that the inhibition zone against *E. coli* and *S. aureus* was about 2 and 3 nm, respectively, which indicates high antibacterial activity. Transmittance spectra (shown in Fig. 8(A)(viii)) of the samples in the UV range (280–400 nm) were also observed to assess the UV-blocking properties. From this figure, it is pretty clear that

the transmittance is very low for AgNP-coated fabrics with and without the OTES layer, which manifests itself as excellent at blocking UV. The sample Cot-Ag-OTES happened to have a UPF (ultraviolet protection factor) value of 266.01 where  $\text{UPF} > 40$  is considered to be excellent against UV radiation. So the fabric produced in this work with a silver nanoparticle coating on cotton mimicking the lotus leaf showed excellent performance as superhydrophobic, anti-bacterial, and UV-blocking fabric.

Bashari *et al.* proposed a natural element-based water repellent nano-coating, instead of using C8 fluorochemical compounds, onto different fabrics using layer by layer self assembly.<sup>85</sup> To replicate the superhydrophobicity observed in nature, various water-repellent finishing agents are used. Among them, fluorocarbons (FCs) possess a unique property of repelling not only water but also oil, providing a surface tension of  $10\text{--}20 \text{ mN m}^{-1}$  while coated on a fabric. However, it has been reported to exert a detrimental effect on the environment and humans leading to the need for alternative green solutions. Carnauba wax obtained from a Brazilian tree carnauba palm, formally known as *Copernicia Prunifera*, is a natural water repellent agent which has been used in this proposed method to develop hydrophobic textiles using layer-by-layer self-assembly. This natural water-repellent nano-coating was deposited on three types of samples, cotton, nylon, and cotton-nylon fabrics. Characterization of the solid carnauba nanoparticles was performed through various measurements and experiments. Table 2 shows the contact angles and the antibacterial effects of the

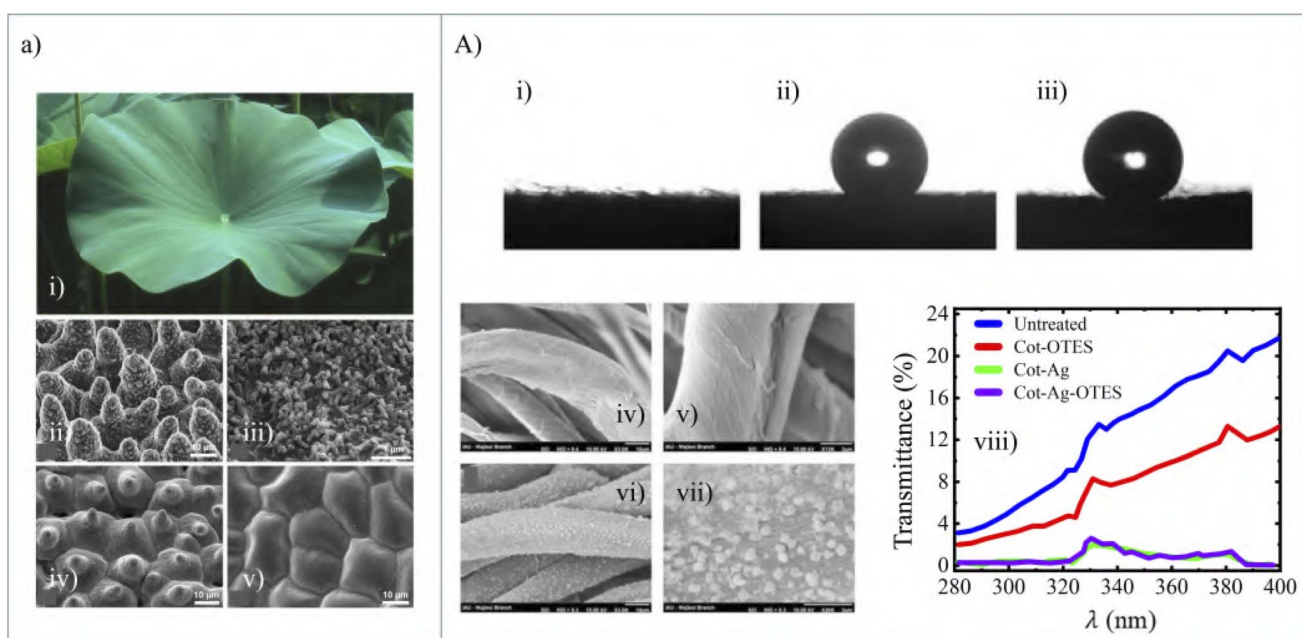


Fig. 8 (a) (i) A natural super-hydrophobic surface lotus leaf (ii) SEM image of the upper leaf side prepared by ‘glycerol substitution’ with the hierarchical surface structure consisting of papillae, wax clusters, and wax tubules. (iii) Wax tubules on the upper leaf side. (iv) Upper leaf side after critical-point (CP) drying and dissolution of wax tubules, which make the stomata visible. (v) CP dried underside leaf shows convex cells without stomata [figure reproduced from ref. 82 with permission from Ensikat *et al.*, copyright 2011]. (A) A 5  $\mu\text{L}$  water droplet on the surface of (i) untreated (ii) the Cot-OTES (iii) Cot-Ag-OTES samples. It is observed from these figures that with Ag coating the contact angle is greater than that of the other two and it shows superhydrophobicity. This is inspired by the superhydrophobicity of the lotus leaf. SEM figure of (iv) and (v) untreated and (vi) and (vii) Cot-Ag samples. The water droplets are seen in the cases of (vi) and (vii). (viii) UV-transmission spectra for different types of cotton samples. The UV blocking performance is better in the case of Ag-coated samples [figure reproduced from ref. 84 with permission from Taylor & Francis Group, copyright 2013].



**Table 2** Contact angle and antibacterial effect of different samples with water as the wetting medium<sup>85</sup>

Sample	Treatment	Averaged contact angle (degree)		Antibacterial effect (%)	
		0 s	30 s	<i>S. aureus</i>	<i>E. coli</i>
Cotton	Untreated	45.36	0	—	—
	Treated	127.6	130.9	95.75	95.1
	Treated after washing	109.9	101.7	—	—
Nyco	Untreated	141.6	48.7	—	—
	Treated	132.1	135	95.75	94.6
	Treated after washing	122.8	124.9	—	—
Nylon 6	Untreated	128.6	77.3	—	—
	Treated	127	131.4	97.78	94.1
	Treated after washing	105.2	102.4	—	—

untreated and treated samples. It is seen that all of the treated samples have significant hydrophobicity for 30 s and even after washing. The coated fabrics show enhanced antibacterial effects against *Staphylococcus aureus* (*S. aureus*) and *Escherichia coli* (*E. coli*). The coated fabrics also show good air permeability and thus have paved the way for green ingredient-based environmentally friendly water repellent textiles.

## 7.2 Textile dyeing

Natural instances show a great variety of structural colors that inspired engineers and designers to design various dyeing techniques and processes. Biomass pigments, with their sustainability, naturality, and biocompatibility, have become an interesting research object in cleaner production-focused textile dyeing. Microbial pigments have the advantage of not being constrained by season, climate, or geography.<sup>198–204</sup> Prodigiosin, an intracellular metabolite with a pyrrole structure, has bright colors and an antibacterial function, making it attractive to the researchers.<sup>86,87</sup> In the past, the pyrrole structure red pigment was insoluble in water and organic solvents had to be used to extract it from the interior of thalli which increased the cost.<sup>205,206</sup> Now, if the pyrrole structure pigment is produced by cell metabolism, it will result in cost reduction and extraction of microbial pigments can be avoided.<sup>88</sup> To design this *trans*-membrane culture, it is required to mimic the mechanism and substance transport through the cell membrane. Through the simulation of an artificial membrane, the chemistry of the preparation and kinetic study of the actual cell membrane can be conducted. Phospholipid bilayers are dynamic and closely similar to cell membranes, and this can be used to research *trans*-membrane behavior. These phospholipid membrane microbial pigments can cross the membrane easily for smaller molecular structure media.<sup>88</sup> It was found in the work presented in ref. 88 for positively charged substances that the pigments had a better mass transfer rate than negatively charged segments. The application of electric fields also boosted the extracellular substance concentration. Using a permeability agent also improved the permeability of pigments.

## 8 Conclusion

This article provides a comprehensive review of how different biological instances have contributed to a number of subfields within the area of nanotechnology, including nanosensors, nanomedicine, nanorobots, nanoenergy harvesting, nanophotonics, and nanotextiles. We briefly discussed how biomimicry led to the invention of several cost-efficient nanosensors with different notable features.

Further applications of biomimicry in the field of nanomedicine and nano-robots to provide assistance in surgery, tissue engineering and drug delivery to different sites of human body have been discussed in adequate detail. Biomimetic innovations have also contributed to the development of novel methods and enhancement of existing ones to harness energy from natural sources to meet the ever increasing demand for eco-friendly green energy. Later we discussed the ways bio-aided innovations have contributed to the development of different nano-photonic structures which significantly improves the performance of solar cells and other such optical devices. Finally, the role of biomimetic nanotechnology in the field of textile engineering has been described to develop superior performing fabric and dyeing pigments compared to the conventional ones.

It should be noted that this review touches on almost all the recent biomimetic innovations and ideas developed in the field of nanosensors, nano-medicine, nano-robots, nano-energy harvesting, nano-photonics and textile engineering. Nevertheless, the studies presented here provide a glimpse into the vast possibilities of biomimicry. According to a study in 2016, the estimated number of living species on Earth ranges from 2 million to 1 trillion, of which approximately 1.74 million have been catalogued.<sup>207,208</sup> So, more than 80 percent of the living creatures have not yet been described. Each of these organisms possesses unique physiological and exterior characteristics to perform distinct functions. Furthermore, these species are constantly evolving over time to adapt to the ever changing nature. Hence, the scope of taking inspirations for novel innovations and improving current ones is infinite. Consequently, the potential applications of biomimicry are limitless. We deem that biologists will discover more astounding information from this vast number of existing species in the future and nanotech researchers will utilize them to build a better future for human civilization.

## Author contributions

The authors confirm their contribution to the paper as follows: conceptualization M. H. H., B. S., T. A. and S. M. C., writing—original draft, literature review, data collection, figure preparation and referencing M. H. H., B. S. and T. A., review and editing, supervision S. M. C. All authors have read and agreed to the published version of the manuscript.

## Conflicts of interest

The authors declare no conflicts of interest.



## Acknowledgements

The authors acknowledge the support of both the Department of Electrical and Electronic Engineering, Bangladesh University of Engineering and Technology, Dhaka, Bangladesh, and the Department of Computer Science and Engineering, Brac University, Dhaka, Bangladesh.

## Notes and references

- J. F. Vincent, O. A. Bogatyreva, N. R. Bogatyrev, A. Bowyer and A.-K. Pahl, *J. R. Soc., Interface*, 2006, **3**, 471–482.
- O. H. Schmitt, *Some Interesting and Useful Biomimetic Transforms, Proceeding*, Third International Biophysics Congress, Boston, Mass., 1969, p. 297.
- D. P. Pulsifer, A. Lakhtakia, R. J. Martín-Palma and C. G. Pantano, *Bioinspiration Biomimetics*, 2010, **5**, 036001.
- R. J. Martín-Palma and A. Lakhtakia, *Int. J. Smart Nano Mater.*, 2013, **4**, 83–90.
- M. Simovic-Pavlovic, B. Bokic, D. Vasiljevic and B. Kolaric, *Appl. Sci.*, 2022, **12**, 905.
- H. Droogendijk, M. J. de Boer, R. G. Sanders and G. J. Krijnen, *J. R. Soc., Interface*, 2014, **11**, 20140438.
- M. Asadnia, A. G. P. Kottapalli, J. Miao, M. E. Warkiani and M. S. Triantafyllou, *J. R. Soc., Interface*, 2015, **12**, 20150322.
- S. Karthick and A. Sen, *Phys. Rev. Appl.*, 2018, **10**, 034037.
- F. Khoshnoud and C. W. de Silva, *IEEE Instrum. Meas. Mag.*, 2012, **15**, 14–24.
- M. Kruusmaa, P. Fiorini, W. Megill, M. de Vittorio, O. Akanyeti, F. Visentin, L. Chambers, H. El Daou, M.-C. Fiazza, J. Ježov, *et al.*, *IEEE Robot. Autom. Mag.*, 2014, **21**, 51–62.
- J. Song, R. Wang, G. Zhang, Z. Shang, L. Zhang and W. Zhang, *IEEE Access*, 2019, **7**, 102366–102376.
- A. Rahaman, H. Jung and B. Kim, *Appl. Sci.*, 2021, **11**, 1305.
- P. P. Vijayan and D. Puglia, *Emergent Mater.*, 2019, **2**, 391–415.
- L. Zhang and T. J. Webster, *Nano Today*, 2009, **4**, 66–80.
- E.-S. Kim, E. H. Ahn, T. Dvir and D.-H. Kim, *Int. J. Nanomed.*, 2014, **9**, 1.
- T. Li, X. Qin, Y. Li, X. Shen, S. Li, H. Yang, C. Wu, C. Zheng, J. Zhu, F. You, *et al.*, *Front. Bioeng. Biotechnol.*, 2020, **8**, 371.
- C. Guido, G. Maiorano, B. Cortese, S. D'Amone and I. E. Palamà, *Bioengineering*, 2020, **7**, 111.
- Z. Jakšić and O. Jakšić, *Biomimetics*, 2020, **5**, 24.
- A. Giwa, S. Hasan, A. Yousuf, S. Chakraborty, D. Johnson and N. Hilal, *Desalination*, 2017, **420**, 403–424.
- R. Bogue, *Assemb. Autom.*, 2008, **28**, 282–288.
- N. Soudi, S. Nanayakkara, N. M. Jahed and S. Naahidi, *Sol. Energy*, 2020, **208**, 31–45.
- Y. Saylan, Ö. Erdem, F. Inci and A. Denizli, *Biomimetics*, 2020, **5**, 20.
- S. Rauf, M. A. Hayat Nawaz, M. Badea, J. L. Marty and A. Hayat, *Sensors*, 2016, **16**, 1931.
- Q. Shen, Z. Luo, S. Ma, P. Tao, C. Song, J. Wu, W. Shang and T. Deng, *Adv. Mater.*, 2018, **30**, 1707632.
- S. A. Frost, C. Wright and M. A. Khan, *AIAA Guidance, Navigation, and Control Conference*, 2015, p. 0083.
- R. Hanlon, *Curr. Biol.*, 2007, **17**, R400–R404.
- H. Schmitz and H. Bousack, *PLoS One*, 2012, **7**, e37627.
- K. Kertész, G. Piszter, Z. Bálint and L. P. Biró, *Sensors*, 2018, **18**, 4282.
- Y. Cui, S. N. Kim, R. R. Naik and M. C. McAlpine, *Acc. Chem. Res.*, 2012, **45**, 696–704.
- J. Park, Y. Lee, J. Hong, Y. Lee, M. Ha, Y. Jung, H. Lim, S. Y. Kim and H. Ko, *ACS Nano*, 2014, **8**, 12020–12029.
- J. C. Breger, C. Yoon, R. Xiao, H. R. Kwag, M. O. Wang, J. P. Fisher, T. D. Nguyen and D. H. Gracias, *ACS Appl. Mater. Interfaces*, 2015, **7**, 3398–3405.
- C. Yoon, *Nano Convergence*, 2019, **6**, 1–14.
- J. D. Hartgerink, E. Beniash and S. I. Stupp, *Science*, 2001, **294**, 1684–1688.
- J. A. Matthews, G. E. Wnek, D. G. Simpson and G. L. Bowlin, *Biomacromolecules*, 2002, **3**, 232–238.
- C. Li, C. Vepari, H. J. Jin, H. J. Kim and D. L. Kaplan, *Biomaterials*, 2006, **27**, 3115–3124.
- G. E. Wnek, M. E. Carr, D. G. Simpson and G. L. Bowlin, *Nano Lett.*, 2003, **3**, 213–216.
- E. D. Boland, G. E. Wnek, D. G. Simpson, K. J. Pawlowski and G. L. Bowlin, *J. Macromol. Sci., Pure Appl. Chem.*, 2001, **38A**, 1231–1243.
- M. Liu, X. Zeng, C. Ma, H. Yi, Z. Ali, X. Mou, S. Li, Y. Deng and N. He, *Bone Res.*, 2017, **5**, 1–20.
- H. Yamaoka, H. Asato, T. Ogasawara, S. Nishizawa, T. Takahashi, T. Nakatsuka, I. Koshima, K. Nakamura, H. Kawaguchi, U. I. Chung, T. Takato and K. Hoshi, *J. Biomed. Mater. Res., Part A*, 2006, **78**, 1–11.
- R. L. Mauck, M. A. Soltz, C. C. Wang, D. D. Wong, P. H. G. Chao, W. B. Valhmu, C. T. Hung and G. A. Ateshian, *J. Biomech. Eng.*, 2000, **122**, 252–260.
- K. Amin, R. Moscalu, A. Imere, R. Murphy, S. Barr, Y. Tan, R. Wong, P. Sorooshian, F. Zhang, J. Stone, J. Fildes, A. Reid and J. Wong, *Nanomedicine*, 2019, **14**, 2679–2696.
- N. M. Molino, A. K. Anderson, E. L. Nelson and S. W. Wang, *ACS Nano*, 2013, **7**, 9743–9752.
- D. P. Patterson, A. Rynda-Apple, A. L. Harmsen, A. G. Harmsen and T. Douglas, *ACS Nano*, 2013, **7**, 3036–3044.
- E. J. Lee, N. K. Lee and I.-S. Kim, *Adv. Drug Delivery Rev.*, 2016, **106**, 157–171.
- J. Ali, U. K. Cheang, J. D. Martindale, M. Jabbarzadeh, H. C. Fu and M. Jun Kim, *Sci. Rep.*, 2016, **7**, 1–10.
- B. Esteban-Fernández de Ávila, P. Angsantikul, D. E. Ramírez-Herrera, F. Soto, H. Teymourian, D. Dehaini, Y. Chen, L. Zhang and J. Wang, *Sci. Robot.*, 2018, **3**(18), eaat0485.
- J. Li, P. Angsantikul, W. Liu, B. Esteban-Fernández de Ávila, X. Chang, E. Sandraz, Y. Liang, S. Zhu, Y. Zhang, C. Chen, *et al.*, *Adv. Mater.*, 2018, **30**, 1704800.
- B. Chen, Z. Zhang, S. Kim, M. Baek, D. Kim and K. Yong, *Appl. Catal., B*, 2019, **259**, 118017.
- G. P. Smestad and M. Gratzel, *J. Chem. Educ.*, 1998, **75**, 752.



50 C. Bhuvaneswari, R. Rajeswari, C. Kalaiarasan and K. Muthukumararajaguru, *Int. J. Sci. Res. Publ.*, 2013, **3**, 1.

51 K. V. Kumar, G. A. Kumar and G. A. K. Reddy, *Caribb. J. Sci. Technol.*, 2014, **2**, 424–430.

52 W. Zhang, D. Zhang, T. Fan, J. Gu, J. Ding, H. Wang, Q. Guo and H. Ogawa, *Chem. Mater.*, 2009, **21**, 33–40.

53 F. Chiadini, V. Fiumara, A. Scaglione and A. Lakhtakia, *Bioinspiration Biomimetics*, 2010, **6**, 014002.

54 R. J. Martín-Palma and A. Lakhtakia, *Int. J. Smart Nano Mater.*, 2013, **4**, 83–90.

55 S. Cui, Y. Zheng, J. Liang and D. Wang, *Nano Res.*, 2018, **11**, 1873–1882.

56 C. He, W. Zhu, G. Q. Gu, T. Jiang, L. Xu, B. D. Chen, C. B. Han, D. Li and Z. L. Wang, *Nano Res.*, 2018, **11**, 1157–1164.

57 J. He, T. Wen, S. Qian, Z. Zhang, Z. Tian, J. Zhu, J. Mu, X. Hou, W. Geng, J. Cho, *et al.*, *Nano Energy*, 2018, **43**, 326–339.

58 D. Y. Kim, H. S. Kim, D. S. Kong, M. Choi, H. B. Kim, J.-H. Lee, G. Murillo, M. Lee, S. S. Kim and J. H. Jung, *Nano Energy*, 2018, **45**, 247–254.

59 C. Xu, Y. Zi, A. C. Wang, H. Zou, Y. Dai, X. He, P. Wang, Y.-C. Wang, P. Feng, D. Li, *et al.*, *Adv. Mater.*, 2018, **30**, 1706790.

60 N. Wang, J. Zou, Y. Yang, X. Li, Y. Guo, C. Jiang, X. Jia and X. Cao, *Nano Energy*, 2019, **55**, 541–547.

61 Y. F. Huang and S. Chattopadhyay, *J. Nanophotonics*, 2013, **7**, 073594.

62 K. Forberich, G. Dennler, M. C. Scharber, K. Hingerl, T. Fromherz and C. J. Brabec, *Thin Solid Films*, 2008, **516**, 7167–7170.

63 J. Zhu, Z. Yu, S. Fan and Y. Cui, *Mater. Sci. Eng., R*, 2010, **70**, 330–340.

64 W. Yi, D.-B. Xiong and D. Zhang, *Nano Adv.*, 2016, **1**, 62–70.

65 M. Yu, Y.-Z. Long, B. Sun and Z. Fan, *Nanoscale*, 2012, **4**, 2783–2796.

66 J. Chen, W.-L. Chang, C. Huang and K. Sun, *Opt. Express*, 2011, **19**, 14411.

67 W. Lan, D. Chen, Q. Guo, B. Tian, X. Xie, Y. He, W. Chai, G. Liu, P. Dong, H. Xi, *et al.*, *Nanomaterials*, 2021, **11**, 2726.

68 S. Ju, M. Byun, M. Kim, J. Jun, D. Huh, D. S. Kim, Y. Jo and H. Lee, *Nano Res.*, 2020, **13**, 1156–1161.

69 W. Qarony, M. I. Hossain, R. Dewan, S. Fischer, V. B. Meyer-Rochow, A. Salleo, D. Knipp and Y. H. Tsang, *Adv. Theory Simul.*, 2018, **1**, 1800030.

70 F. Tao, P. Hiralal, L. Ren, Y. Wang, Q. Dai, G. A. Amaratunga and H. Zhou, *Nanoscale Res. Lett.*, 2014, **9**, 1–7.

71 J. Sun, X. Wang, J. Wu, C. Jiang, J. Shen, M. A. Cooper, X. Zheng, Y. Liu, Z. Yang and D. Wu, *Sci. Rep.*, 2018, **8**, 1–10.

72 M.-c. Kim, S. Jang, J. Choi, S. M. Kang and M. Choi, *Nano-Micro Lett.*, 2019, **11**, 1–10.

73 S. Ji, K. Song, T. B. Nguyen, N. Kim and H. Lim, *ACS Appl. Mater. Interfaces*, 2013, **5**, 10731–10737.

74 H.-W. Yun, G.-M. Choi, H. K. Woo, S. J. Oh and S.-H. Hong, *Curr. Appl. Phys.*, 2020, **20**, 1163–1170.

75 V. R. Binetti, J. D. Schiffman, O. D. Leaffer, J. E. Spanier and C. L. Schauer, *Integr. Biol.*, 2009, **1**, 324–329.

76 R. H. Siddique, G. Gomard and H. Hölscher, *Nat. Commun.*, 2015, **6**, 1–8.

77 J. Morikawa, M. Ryu, G. Seniutinas, A. Balcytis, K. Maximova, X. Wang, M. Zamengo, E. P. Ivanova and S. Juodkazis, *Langmuir*, 2016, **32**, 4698–4703.

78 A. Papadopoulos, E. Skoulas, A. Mimidis, G. Perrakis, G. Kenanakis, G. D. Tsibidis and E. Stratakis, *Adv. Mater.*, 2019, **31**, 1901123.

79 A. Marmur, *Langmuir*, 2004, **20**, 3517–3519.

80 L. Zhang, Z. Zhou, B. Cheng, J. M. DeSimone and E. T. Samulski, *Langmuir*, 2006, **22**, 8576–8580.

81 K. Balani, R. G. Batista, D. Lahiri and A. Agarwal, *Nanotechnology*, 2009, **20**, 305707.

82 H. J. Ensikat, P. Ditsche-Kuru, C. Neinhuis and W. Barthlott, *Beilstein J. Nanotechnol.*, 2011, **2**, 152–161.

83 S. Das, N. Shanmugam, A. Kumar and S. Jose, *Bioinspired, Biomimetic Nanobiomater.*, 2017, **6**, 224–235.

84 M. Shateri-Khalilabad and M. E. Yazdanshenas, *J. Text. Inst.*, 2013, **104**, 861–869.

85 A. Bashari, A. H. Salehi K and N. Salamatipour, *J. Text. Inst.*, 2020, **111**, 1148–1158.

86 X. Liu, Y. Wang, S. Sun, C. Zhu, W. Xu, Y. Park and H. Zhou, *Prep. Biochem. Biotechnol.*, 2013, **43**, 271–284.

87 O. Falklöf and B. Durbeej, *ChemPhysChem*, 2016, **17**, 954–957.

88 J. Gong, J. Liu, X. Tan, Z. Li, Q. Li and J. Zhang, *Nanomaterials*, 2019, **9**, 114.

89 A. Munawar, Y. Ong, R. Schirhagl, M. A. Tahir, W. S. Khan and S. Z. Bajwa, *RSC Adv.*, 2019, **9**, 6793–6803.

90 S. A. Perdomo, J. M. Marmolejo-Tejada and A. Jaramillo-Botero, *J. Electrochem. Soc.*, 2021, **168**, 107506.

91 A. K. Srivastava, A. Dev and S. Karmakar, *Environ. Chem. Lett.*, 2018, **16**, 161–182.

92 P. J. Vikesland, *Nat. Nanotechnol.*, 2018, **13**, 651–660.

93 N. Elhardt, Self-published photo. From Wikimedia Commons, distributed under a CC BY-SA 2.5 license.

94 USDAgov, From Wikimedia Commons, distributed under a CC BY 2.0 license.

95 Webridge, From Wikimedia Commons, distributed under a CC BY-SA 3.0 license.

96 B. Blaus, Medical Gallery of Blausen Medical 2014, *Wiki. J. Med.*, **1** (2), DOI: [10.15347/wjm/2014.010](https://doi.org/10.15347/wjm/2014.010). ISSN 2002-4436. Own work, distributed under a CC BY 3.0.

97 R. J. Martín-Palma and M. Kolle, *Opt. Laser Technol.*, 2019, **109**, 270–277.

98 H. Herzog, A. Klein, H. Bleckmann, P. Holik, S. Schmitz, G. Siebke, S. Tätzner, M. Lacher and S. Steltenkamp, *Bioinspiration Biomimetics*, 2015, **10**, 036001.

99 R. A. Potyrailo, H. Ghiradella, A. Vertiatchikh, K. Dovidenko, J. R. Cournoyer and E. Olson, *Nat. Photonics*, 2007, **1**, 123–128.

100 Y. Lee, J. Park, A. Choe, S. Cho, J. Kim and H. Ko, *Adv. Funct. Mater.*, 2020, **30**, 1904523.

101 Y. Lee and J.-H. Ahn, *ACS Nano*, 2020, **14**, 1220–1226.

102 G. Wu, C. Feng, J. Quan, Z. Wang, W. Wei, S. Zang, S. Kang, G. Hui, X. Chen and Q. Wang, *Carbohydr. Polym.*, 2018, **182**, 215–224.



103 M. M. Martino, S. Brkic, E. Bovo, M. Burger, D. J. Schaefer, T. Wolff, L. Gürke, P. S. Briquez, H. M. Larsson, R. Gianni Barrera, *et al.*, *Front. Bioeng. Biotechnol.*, 2015, **3**, 45.

104 D. Girard, B. Laverdet, V. Buhé, M. Trouillas, K. Ghazi, M. M. Alexaline, C. Egles, L. Misery, B. Coulomb, J.-J. Lataillade, *et al.*, *Tissue Eng., Part B*, 2017, **23**, 59–82.

105 B. Weyand and P. Vogt, *Biomimetics and Bionic Applications with Clinical Applications*, Springer, 2021, pp. 29–43.

106 J. Du, H. Chen, L. Qing, X. Yang and X. Jia, *Biomater. Sci.*, 2018, **6**, 1299–1311.

107 M. Olsson, P. Bruhns, W. A. Frazier, J. V. Ravetch and P. A. Oldenborg, *Blood*, 2005, **105**, 3577–3582.

108 P. Sims, S. Rollins and T. Wiedmer, *J. Biol. Chem.*, 1989, **264**, 19228–19235.

109 J. Li, P. Angsantikul, W. Liu, B. Esteban-Fernández de Ávila, X. Chang, E. Sandraz, Y. Liang, S. Zhu, Y. Zhang, C. Chen, W. Gao, L. Zhang and J. Wang, *Adv. Mater.*, 2018, **30**, 1–8.

110 S. Barr and A. Bayat, *Aesthetic Surg. J.*, 2011, **31**, 56–67.

111 S. Barr, E. W. Hill and A. Bayat, *Acta Biomater.*, 2017, **49**, 260–271.

112 P. X. Ma, *Adv. Drug Delivery Rev.*, 2008, **60**, 184–198.

113 E. Brett, J. Flacco, C. Blackshear, M. T. Longaker and D. C. Wan, *BioRes. Open Access*, 2017, **6**, 1–6.

114 D. W. Buck, G. A. Dumanian, *et al.*, *Plast. Reconstr. Surg.*, 2012, **129**, 950e–956e.

115 R. Verboket, M. Leiblein, C. Seebach, C. Nau, M. Janko, M. Bellen, H. Bönig, D. Henrich and I. Marzi, *Eur. J. Trauma Emerg. Surg.*, 2018, **44**, 649–665.

116 F. M. Wood, *Int. J. Biochem. Cell Biol.*, 2014, **56**, 133–140.

117 R. H. Fang, Y. Jiang, J. C. Fang and L. Zhang, *Biomaterials*, 2017, **128**, 69–83.

118 J. E. Bernth, A. Arezzo and H. Liu, *IEEE Rob. Autom. Lett.*, 2017, **2**, 1718–1724.

119 B. E. F. De Ávila, P. Angsantikul, D. E. Ramírez-Herrera, F. Soto, H. Teymourian, D. Dehaini, Y. Chen, L. Zhang and J. Wang, *Sci. Robot.*, 2018, **3**, 485.

120 Y. Lu, Q. Hu, C. Jiang and Z. Gu, *Curr. Opin. Biotechnol.*, 2019, **58**, 81–91.

121 R. Hille, Distributed under a CC BY-SA 3.0 license, <https://candide.com/GB/insects/607a3d43-0eb0-4100-8f0f-43117cb332a0>.

122 Y. Li and C. Liu, *Nanoscale*, 2017, **9**, 4862–4874.

123 A. Khademhosseini and R. Langer, *Nat. Protoc.*, 2016, **11**, 1775–1781.

124 Y. Zhao, C. Shi, X. Yang, B. Shen, Y. Sun, Y. Chen, X. Xu, H. Sun, K. Yu, B. Yang, *et al.*, *ACS Nano*, 2016, **10**, 5856–5863.

125 H. Haidari, K. Vasilev, A. J. Cowin and Z. Kopecki, *ACS Appl. Mater. Interfaces*, 2022, **14**(46), 51744–51762.

126 N. Huebsch, C. J. Kearney, X. Zhao, J. Kim, C. A. Cezar, Z. Suo and D. J. Mooney, *Proc. Natl. Acad. Sci. U. S. A.*, 2014, **111**, 9762–9767.

127 A. Schroeder, Y. Avnir, S. Weisman, Y. Najajreh, A. Gabizon, Y. Talmon, J. Kost and Y. Barenholz, *Langmuir*, 2007, **23**, 4019–4025.

128 A. Schroeder, R. Honen, K. Turjeman, A. Gabizon, J. Kost and Y. Barenholz, *J. Controlled Release*, 2009, **137**, 63–68.

129 H. Epstein-Barash, G. Orbey, B. E. Polat, R. H. Ewoldt, J. Feshitan, R. Langer, M. A. Borden and D. S. Kohane, *Biomaterials*, 2010, **31**, 5208–5217.

130 Q. Lin, Q. Huang, C. Li, C. Bao, Z. Liu, F. Li and L. Zhu, *J. Am. Chem. Soc.*, 2010, **132**, 10645–10647.

131 R. M. Baxter, T. Dai, J. Kimball, E. Wang, M. R. Hamblin, W. P. Wiesmann, S. J. McCarthy and S. M. Baker, *J. Biomed. Mater. Res., Part A*, 2013, **101**, 340–348.

132 E. M. Ahmed, *J. Adv. Res.*, 2015, **6**, 105–121.

133 A. Ummat, A. Dubey and C. Mavroidis, *Biomimetics: Biologically Inspired Technologies*, CRC Press, Boca Raton, FL, 2005, pp. 201–227.

134 D. G. Beards, From Wikimedia Commons, distributed under a CC BY-SA 4.0 license.

135 B. Wetzel and H. Schaefer, National Cancer Institute., 1982, retrieved from, <https://visualsonline.cancer.gov/details.cfm?imageid=2129>.

136 J. Ali, U. K. Cheang, J. D. Martindale, M. Jabbarzadeh, H. C. Fu and M. Jun Kim, *Sci. Rep.*, 2017, **7**, 1–10.

137 L. Roberts, *9 Billion?*, 2011.

138 N. S. Lewis and D. G. Nocera, *Proc. Natl. Acad. Sci. U. S. A.*, 2006, **103**, 15729–15735.

139 A. Hassan, S. Z. Ilyas, A. Jalil and Z. Ullah, *Environ. Sci. Pollut. Res.*, 2021, **28**, 21204–21211.

140 W. Bank, *Pakistan Strategic Country Environmental Assessment*, 2006.

141 K. B. Karnauskas, S. L. Miller and A. C. Schapiro, *GeoHealth*, 2020, **4**(5), e2019GH000237.

142 F. Perera, *Int. J. Environ. Res. Public Health*, 2018, **15**, 16.

143 L. Allen, M. J. Cohen, D. Abelson and B. Miller, *The World's Water*, Springer, 2012, pp. 73–96.

144 J. M. Navas, M. Babín, S. Casado, C. Fernández and J. V. Tarazona, *Mar. Environ. Res.*, 2006, **62**, S352–S355.

145 N. Butt, H. Beyer, J. Bennett, D. Biggs, R. Maggini, M. Mills, A. Renwick, L. Seabrook and H. Possingham, *Science*, 2013, **342**, 425–426.

146 S. Wylie, E. Wilder, L. Vera, D. Thomas and M. McLaughlin, *Sci. Technol. Soc.*, 2017, **3**, 426.

147 M. B. Harfoot, D. P. Tittensor, S. Knight, A. P. Arnell, S. Blyth, S. Brooks, S. H. Butchart, J. Hutton, M. I. Jones, V. Kapos, *et al.*, *Conserv. Lett.*, 2018, **11**, e12448.

148 S. Shafiee and E. Topal, *Energy Policy*, 2009, **37**, 181–189.

149 C. J. Barbe, F. Arendse, P. Comte, M. Jirousek, F. Lenzmann, V. Shklover and M. Grätzel, *J. Am. Ceram. Soc.*, 1997, **80**, 3157–3171.

150 S. Hore, P. Nitz, C. Vetter, C. Prahl, M. Niggemann and R. Kern, *Chem. Commun.*, 2005, 2011–2013.

151 Z.-S. Wang, H. Kawauchi, T. Kashima and H. Arakawa, *Coord. Chem. Rev.*, 2004, **248**, 1381–1389.

152 J. Ren, Q. Liu, Y. Pei, Y. Wang, S. Yang, S. Lin, W. Chen, S. Ling and D. L. Kaplan, *Adv. Mater. Technol.*, 2021, **6**, 2001301.

153 T. Wang and T. F. Ciszek, Purified silicon production system, *US Pat.*, US6712908B2, 2004, <https://patents.google.com/patent/US6712908>.

154 S. Ali and J. Matthew, Biomimicry in Solar Energy Conversion with Natural Dye Sensitized Nanocrystalline



Photovoltaic Cells, Post graduate thesis, Department of Chemistry and Biochemistry Obelin College, Ohio, 2007, pp. 1–22.

155 T. W. Hamann, R. A. Jensen, A. B. Martinson, H. Van Ryswyk and J. T. Hupp, *Energy Environ. Sci.*, 2008, **1**, 66–78.

156 A. Yella, H.-W. Lee, H. N. Tsao, C. Yi, A. K. Chandiran, M. K. Nazeeruddin, E. W.-G. Diau, C.-Y. Yeh, S. M. Zakeeruddin and M. Grätzel, *Science*, 2011, **334**, 629–634.

157 W. Yan, Y. Huang, L. Wang, F. Vuellers, M. N. Kavalenka, H. Hoelscher, S. Dottermusch, B. S. Richards and E. Klampaftis, *Sol. Energy Mater. Sol. Cells*, 2018, **186**, 105–110.

158 S. Das, M. J. Hossain, S.-F. Leung, A. Lenox, Y. Jung, K. Davis, J.-H. He and T. Roy, *Nano Energy*, 2019, **58**, 47–56.

159 Z. L. Wang, *Faraday Discuss.*, 2015, **176**, 447–458.

160 Q. Schiermeier, *Nature*, 2016, **535**, 212–214.

161 J. Wang, S. Li, F. Yi, Y. Zi, J. Lin, X. Wang, Y. Xu and Z. L. Wang, *Nat. Commun.*, 2016, **7**, 1–8.

162 B. Sørensen, *Nature*, 2017, **543**, 491.

163 Z. L. Wang, *Nature*, 2017, **542**, 159–160.

164 S. Save and K. Mishra, *Int. J. Comput. Appl.*, 2015, **975**, 8887.

165 D. Bogdanov and C. Breyer, *Proceedings of the 19th Sede Boqer Symposium on Solar Electricity Production February 23–25, 2015*, 2015.

166 X. Zhou, J. Zhang, Q. Su, J. Shi, Y. Liu and G. Du, *Electrochim. Acta*, 2014, **125**, 615–621.

167 Tomatito26, <https://www.dreamstime.com/stock-images-macro-fly-compound-eye-surface-magnification-image29981764>.

168 R. Cowen, <https://physicsworld.com/a/moth-eyes-inspire-more-efficient-solar-cell/>.

169 S. J. Wright, [https://academic.udayton.edu/shirleywright/sem/images/Samples/SEM\\_MothEye.jpg](https://academic.udayton.edu/shirleywright/sem/images/Samples/SEM_MothEye.jpg).

170 S. Ji, J. Park and H. Lim, *Nanoscale*, 2012, **4**, 4603–4610.

171 W. Distant, <https://www.cicadamania.com/cicadas/category/researchers/william-lucas-distant/page/3/>.

172 M. Sun, A. Liang, G. S. Watson, J. A. Watson, Y. Zheng, J. Ju and L. Jiang, *PLoS One*, 2012, **7**, e35056.

173 A. R. Parker and H. E. Townley, *Nat. Nanotechnol.*, 2007, **2**, 347–353.

174 P. Vukusic and J. R. Sambles, *Nature*, 2003, **424**, 850–855.

175 J. Xu and Z. Guo, *J. Colloid Interface Sci.*, 2013, **406**, 1–17.

176 H. Ghiradella, *Appl. Opt.*, 1991, **30**, 3492–3500.

177 R. O. Prum and R. Torres, *J. Exp. Biol.*, 2003, **206**, 2409–2429.

178 D. G. Stavenga, H. L. Leertouwer, N. J. Marshall and D. Osorio, *Proc. R. Soc. B*, 2011, **278**, 2098–2104.

179 S. Vignolini, E. Moyroud, B. J. Glover and U. Steiner, *J. R. Soc., Interface*, 2013, **10**, 20130394.

180 N. N. Shi, C.-C. Tsai, F. Camino, G. D. Bernard, N. Yu and R. Wehner, *Science*, 2015, **349**, 298–301.

181 S. Wilson and M. Hutley, *Opt. Acta*, 1982, **29**, 993–1009.

182 C. Bernhard, G. Gemne and G. Seitz, *Physiology of Photoreceptor Organs*, 1972, pp. 357–379.

183 A. Yoshida, M. Motoyama, A. Kosaku and K. Miyamoto, *Zool. Sci.*, 1997, **14**, 737–741.

184 C. Bernhard, *Endeavour*, 1967, **26**, 79–84.

185 P. Clapham and M. Hutley, *Nature*, 1973, **244**, 281–282.

186 A. S. Rad, A. Afshar and M. Azadeh, *Opt. Mater.*, 2020, **107**, 110027.

187 T. Sertel, Y. Ozen, V. Baran and S. Ozcelik, *J. Alloys Compd.*, 2019, **806**, 439–450.

188 J. Choi, *J. Mech. Sci. Technol.*, 2016, **30**, 2707–2711.

189 A. Gombert, W. Glaubitt, K. Rose, J. Dreibholz, B. Bläsi, A. Heinzel, D. Sporn, W. Döll and V. Wittwer, *Sol. Energy*, 2000, **68**, 357–360.

190 P. Yu, C.-H. Chang, C.-H. Chiu, C.-S. Yang, J.-C. Yu, H.-C. Kuo, S.-H. Hsu and Y.-C. Chang, *Adv. Mater.*, 2009, **21**, 1618–1621.

191 A. Jannasch, A. F. Demirörs, P. D. Van Oostrum, A. Van Blaaderen and E. Schäffer, *Nat. Photonics*, 2012, **6**, 469–473.

192 D. Gao, W. Ding, M. Nieto-Vesperinas, X. Ding, M. Rahman, T. Zhang, C. Lim and C.-W. Qiu, *Light: Sci. Appl.*, 2017, **6**, e17039.

193 J.-Q. Xi, M. F. Schubert, J. K. Kim, E. F. Schubert, M. Chen, S.-Y. Lin, W. Liu and J. A. Smart, *Nat. Photonics*, 2007, **1**, 176–179.

194 Z. Diao, M. Kraus, R. Brunner, J.-H. Dirks and J. P. Spatz, *Nano Lett.*, 2016, **16**, 6610–6616.

195 K. Pfeiffer, U. Schulz, A. Tünnermann and A. Szeghalmi, *Coatings*, 2017, **7**, 118.

196 R. Lou, G. Zhang, G. Li, X. Li, Q. Liu and G. Cheng, *Micromachines*, 2019, **11**, 20.

197 N. Livakas, E. Skoulas and E. Stratakis, *Opto-Electron. Adv.*, 2020, **3**, 190035.

198 R. Panesar, S. Kaur and P. S. Panesar, *Curr. Opin. Food Sci.*, 2015, **1**, 70–76.

199 A. Kumar, H. S. Vishwakarma, J. Singh, S. Dwivedi and M. Kumar, *Int. J. Pharm., Chem. Biol. Sci.*, 2015, **5**(1), 203–212.

200 H. S. Tuli, P. Chaudhary, V. Beniwal and A. K. Sharma, *J. Food Sci. Technol.*, 2015, **52**, 4669–4678.

201 P. S. Nigam and J. S. Luke, *Curr. Opin. Food Sci.*, 2016, **7**, 93–100.

202 L. Dufosse, M. Fouillaud, Y. Caro, S. A. Mapari and N. Sutthiwong, *Curr. Opin. Biotechnol.*, 2014, **26**, 56–61.

203 C. K. Venil, C. A. Aruldass, L. Dufossé, Z. A. Zakaria and W. A. Ahmad, *RSC Adv.*, 2014, **4**, 39523–39529.

204 C. K. Venil, Z. A. Zakaria and W. A. Ahmad, *Process Biochem.*, 2013, **48**, 1065–1079.

205 F. Alihosseini, K.-S. Ju, J. Lango, B. D. Hammock and G. Sun, *Biotechnol. Prog.*, 2008, **24**, 742–747.

206 Y. Kim and J. Choi, *Fibers Polym.*, 2015, **16**, 1981–1987.

207 K. J. Locey and J. T. Lennon, *Proc. Natl. Acad. Sci. U. S. A.*, 2016, **113**, 5970–5975.

208 C. of Life, 2018, <https://www.catalogueoflife.org/>.

